

# POR-Based Channel Estimation for UWB Communications

Ping Liu, *Member, IEEE*, and Zhengyuan Xu, *Senior Member, IEEE*

**Abstract**—In an ultrawideband (UWB) system, typically, a Rake receiver is employed to detect information symbols. To fully capture signal energy spread over multiple paths, the desired user's channel parameters are necessary. In this paper, we first convert a time-hopping (TH) UWB signal model using pulse position modulation (PPM) to a linear form similar to that of a code division multiple access (CDMA) system. Then, we apply a power-of- $R$  (POR) technique to blindly estimate multipath parameters of the desired user in a multiple-access (MA) UWB system, where “ $R$ ” represents the data covariance matrix. The POR technique is related to the subspace technique in that it directly estimates the unknown noise-subspace component in the subspace method but avoids rank estimation where errors may be incurred by perturbations in practical conditions. Performance of the proposed POR channel estimator is analyzed and shown to converge to that of the ideal subspace approach. Detection performance of the Rake receiver constructed from the estimated channel is also studied in terms of output signal-to-interference-plus-noise ratio (SINR) and bit error rate (BER). The proposed method demonstrates superiority to existing maximum-likelihood (ML)-based approaches in terms of either channel estimation or symbol detection. It also outperforms the subspace method for heavily loaded systems.

**Index Terms**—Channel estimation, perturbation analysis, power of  $R$  (POR), subspace decomposition, ultrawideband (UWB) communication.

## I. INTRODUCTION

THE time-hopping (TH) ultrawideband (UWB) modulation technology has attracted considerable research attention recently, due to its appealing features and the recent release of the spectral mask from the Federal Communications Commission [1]. It is an ideal candidate for secure low-power multiuser communications, since it offers exceptional multipath resolvability, robustness to jamming, and low probability of interception and detection [2].

In a UWB system, a Rake receiver is typically employed to detect information symbols. To fully capture signal energy

spread over multiple paths, channel parameters are necessary to construct a Rake receiver [3]. However, channel information is not known *a priori*, especially in a dense multipath wireless environment. Recently, maximum-likelihood (ML) channel-estimation methods with/without aid of training sequences have been proposed [4], [5], which provide a theoretical guidance for evaluation of other channel estimators. However, ML-based channel-estimation methods are computationally prohibitive. Meanwhile, multiuser interference (MUI) is approximated as a Gaussian process that may lead to degraded performance, especially in a system where intersymbol interference (ISI) and/or MUI are significant. Low-complexity channel estimators with explicit consideration of MUI are thus desirable.

In this paper, we focus on channel estimation in a multiple-access (MA) communication environment, based on up to the second-order statistics (SOSs) of the received signal. First, following [6], a data model similar to a direct-sequence (DS) code division multiple access (CDMA) system is constructed for a TH-UWB system with pulse position modulation (PPM), where each user takes  $M$  virtual inputs corresponding to  $M$  modulation levels. We can define a code matrix for each of the  $M$  virtual inputs corresponding to a user from that user's unique TH sequence and the virtual input's level. If we treat the “code” matrix to be in a similar role as a code matrix in a CDMA system, then the model will be shown to be similar to a multicode multirate CDMA system [7], leading to possible application of a power-of- $R$  (POR) technique [8], [9] with  $R$  denoting the data covariance matrix. Instead of estimating the noise subspace of the data covariance matrix by subspace decomposition in the subspace technique [10], the POR technique [8], [9] approximates the noise-subspace component from the power of the inverse data covariance matrix  $R^{-p}$ , where  $p$  is a positive integer. Asymptotic equivalence between the POR method and the subspace method is established theoretically. Simulation results demonstrate that, with finite received data samples, the POR method based on a small  $p$  behaves as well as the subspace method in favorable communication systems such as those with light loading. However, the former significantly outperforms the latter with medium to heavy loading.

In the UWB model, the received signal shows nonzero mean due to PPM, different from a typical CDMA system where zero-mean inputs yield zero-mean channel output in general. This has been observed in subspace techniques [11], [12] and the minimum-variance technique [13], or even mean and covariance-based channel-estimation methods [14], [15]. Therefore, for convenience, zero-mean data is obtained after subtracting the estimated mean from directly received data. This provides two benefits: 1) easy application of the POR

Manuscript received January 21, 2004; revised July 29, 2004; accepted September 6, 2004. The editor coordinating the review of this paper and approving it for publication is R. Murch. The work of P. Liu was supported by Arkansas Center for Energy, Natural Resources, and Environmental Studies. The work of Z. Xu was supported by the U.S. Army Research Laboratory under the Collaborative Technology Alliance Program, Cooperative Agreement DAAD19-01-2-0011. The U.S. Government is authorized to reproduce and distribute reprints for government purposes notwithstanding any copyright notation thereon. The views and conclusions contained in this document are those of the authors and should not be interpreted as representing the official policies, either expressed or implied, of the Army Research Laboratory or the U.S. Government.

P. Liu is with the Department of Electrical Engineering, Arkansas Tech University, Russellville, AR 72801 USA (e-mail: Ping.Liu@atu.edu).

Z. Xu is with the Department of Electrical Engineering, University of California, Riverside, CA 92521 USA (e-mail: dxu@ee.ucr.edu).

Digital Object Identifier 10.1109/TWC.2005.858360

technique [8]; and 2) performance improvement of linear detectors [16] by significantly reducing the amount of MUI. After mean subtraction and defining multiple virtual inputs for each user, the new model shows similarities to a CDMA system. However, the newly defined input signals are correlated because they stem from the same modulation delay. To successfully apply the POR technique, further transformation on those signals is performed to remove the correlation [11], [13]. Thereafter, adopting a criterion similar to that in the POR technique, channel parameters for the desired user can be estimated by minimizing the projection of the signature waveform onto the power of the inverse data covariance matrix. Then, Rake receivers can be built based on the estimated channel vector. Channel-estimation performance is evaluated when noise is nontrivial and covariance is estimated from finite data samples. Meanwhile, signal-to-interference-plus-noise ratio (SINR) of a Rake receiver is studied jointly with channel estimation. Those results can be used to predict detection performance for given operational conditions. Simulation examples show that the proposed POR method outperforms the ML method [5] in many scenarios. The POR method also outperforms the subspace method in a heavily loaded system.

Some notations following common practice are adopted throughout the paper. We denote Kronecker product [17] by  $\otimes$ , complex conjugate (\*) transpose ( $\text{T}$ ) by  $\text{H}$ , inverse by  $^{-1}$ , pseudoinverse by  $\dagger$ , trace of a matrix by  $\text{tr}(\cdot)$ , and determinant by  $\det(\cdot)$ .  $\text{Re}\{\cdot\}$  represents real part,  $\text{E}\{\cdot\}$  expectation, and  $\mathbf{I}_a$  is an identity matrix of degree  $a$  whose  $i$ th column is denoted by  $\mathbf{e}_{a,i}$ . A vector of length  $a$  with all elements equal to 1 is denoted  $\mathbf{1}_a$ . Integer floor is denoted as  $\lfloor \cdot \rfloor$ , and integer ceil as  $\lceil \cdot \rceil$ . An estimate of a quantity (scalar, vector, or matrix) is denoted by putting a  $\hat{\cdot}$  over it, and correspondingly, the estimation error, by preceding the quantity with a  $\delta$ , such as  $\widehat{\mathbf{X}}$  and  $\delta\mathbf{X}$  for matrix  $\mathbf{X}$ , respectively. Not to be confused with the previous usage, we also use  $\delta(\cdot)$  to represent a discrete-time unit impulse function. A  $Q$  function  $Q(x) = 1/\sqrt{2\pi} \int_x^\infty e^{-t^2/2} dt$  will be used in analyzing detection performance.

## II. DISCRETE-TIME UWB SYSTEM MODEL

Assume there are  $K$  users simultaneously sharing the spectrum in an MA TH-UWB system. The transmitted baseband UWB signal from user  $k$  can be described by [6]

$$\alpha_k(t) = \sqrt{\mathcal{P}_k} \sum_{i=-\infty}^{\infty} w\left(t - iT_f - c_k(i)T_c - \tau_{I_k(\lfloor i/N_f \rfloor)}\right) \quad (1)$$

where  $\mathcal{P}_k$  is the  $k$ th user's transmission power,  $w(t)$  is the baseband monopulse,  $T_f$  is the frame duration,  $N_f$  is the number of frames over which an  $M$ -ary pulse position modulation (PPM) symbol repeats, and  $c_k(i) \in [0, N_c - 1]$  is a periodic hopping sequence with period equal to one symbol period. Each chip has duration  $T_c$ .  $I_k(\lfloor i/N_f \rfloor) \in [0, M - 1]$  is the  $k$ th user's information-bearing symbol during the  $i$ th frame,  $\tau_{I_k(\lfloor i/N_f \rfloor)} = I_k(\lfloor i/N_f \rfloor)\sigma$  is the corresponding modulation delay in multiples of  $\sigma$  seconds. Assume  $T_f = N_c T_c$  and  $T_c = M\sigma$ . Equation (1) shows a nonlinear form between  $\alpha_k(t)$  and the transmitted information symbol. However, a linear relationship can be

obtained, as shown in [6]. Let us define  $M$  virtual inputs for user  $k$  with the  $m$ th one as

$$s_{k,m} \left( \left\lfloor \frac{i}{N_f} \right\rfloor \right) = \delta \left( I_k \left( \left\lfloor \frac{i}{N_f} \right\rfloor \right) - m \right).$$

Clearly, only one of the  $M$  inputs will be nonzero each time. Correspondingly,  $M$  pulse-rate code sequences are defined for the  $M$  virtual inputs with the  $m$ th sequence as  $\mathbf{c}_{k,m} = \tilde{\mathbf{c}}_k \otimes \mathbf{e}_{M,m}$ , where  $\tilde{\mathbf{c}}_k$  is the chip-rate code sequence, with its  $i$ th element defined as

$$\tilde{c}_k(i) = \delta \left( \left\lfloor \frac{i}{N_c} \right\rfloor N_c + c_k \left( \left\lfloor \frac{i}{N_c} \right\rfloor \right) - i \right).$$

Then, (1) can be equivalently expressed as [11], [13]

$$\alpha_k(t) = \sqrt{\mathcal{P}_k} \sum_{i=-\infty}^{\infty} \sum_{m=0}^{M-1} u_{k,m}(i) w(t - i\sigma)$$

where  $u_{k,m}(i) = \sum_{l=-\infty}^{\infty} s_{k,m}(l) c_{k,m}(i - lP)$ ,  $P \triangleq MN_c N_f$ , and  $c_{k,m}(i)$  is the  $i$ th element of  $\mathbf{c}_{k,m}$ . If we define an effective channel including effects from modulated pulse at the transmitter, propagation channel  $\bar{g}_k(t)$ , and matched filter at the receiver by  $g_k(t) = \sqrt{\mathcal{P}_k} w(t) \star \bar{g}_k(t) \star w(-t)$ , where  $\star$  denotes convolution, then the received signal sampled every  $\sigma$  seconds (at pulse rate)

$$y(n) = \sum_{k,m} \sum_{i=0}^q u_{k,m}(n - i - d_k) g_k(i) + v(n) \quad (2)$$

where  $n$ ,  $v(n)$ , and  $d_k$  denote time index, additive white Gaussian noise (AWGN), and propagation delay of user  $k$ , respectively. The effective channel delay spread is assumed to be  $q\sigma$ . If we collect  $\nu = P$  samples from  $y(nP+1), \dots, y(nP+P)$  and put them in  $\mathbf{y}_n$ , then the received data vector follows [13]

$$\mathbf{y}_n = \sum_{k,m,l} \mathbf{C}_{k,m,l} \mathbf{g}_k s_{k,m}(n+l) + \mathbf{v}_n \quad (3)$$

where  $l$  takes all integers from  $-\lceil q/P \rceil$  to 0,  $\mathbf{g}_k$  is an unknown channel vector for user  $k$ , which contains channel coefficients at the pulse rate and power factor  $\sqrt{\mathcal{P}_k}$ , and  $\mathbf{C}_{k,m,l}$  is a code filtering matrix for user  $k$ 's  $m$ th virtual input at delay  $l$ . It is constructed from  $\mathbf{c}_{k,m}$  with some heading and trailing 0's determined by that user's propagation delay. The model (3) can be compactly expressed in another form

$$\mathbf{y}_n = \sum_{k,l} \mathbf{H}_{k,l} \mathbf{s}_{k,n,l} + \mathbf{v}_n = \mathbf{H} \mathbf{s}_n + \mathbf{v}_n \quad (4)$$

after collecting  $M$  inputs in a vector  $\mathbf{s}_{k,n,l} = [s_{k,0}(n+l), \dots, s_{k,M-1}(n+l)]^T$ , defining a corresponding effective channel matrix

$$\mathbf{H}_{k,l} = [\mathbf{C}_{k,0,l} \mathbf{g}_k, \dots, \mathbf{C}_{k,M-1,l} \mathbf{g}_k] \quad (5)$$

and successively stacking such matrices (or vectors) in  $\mathbf{H}$  (or  $\mathbf{s}_n$ ).

### III. BLIND POR-BASED CHANNEL ESTIMATION AND SYMBOL DETECTION

#### A. POR-Based Channel Estimation

In a conventional CDMA system, a data-correlation matrix is applied for POR channel estimation [8], [9]. However, according to (4), the received data  $\mathbf{y}_n$  has nonzero mean, which will induce nonzero cross terms in its correlation matrix and is inconvenient for channel estimation. Therefore, a data covariance matrix is desired. To obtain the data covariance matrix, we first find the mean of the data vector and then subtract it to obtain a zero-mean data vector. Let us make the following widely adopted assumptions [5].

- 1) Users' inputs are independent and identically distributed.
- 2) The additive noise has zero mean.
- 3) Each user's TH sequence repeats from symbol to symbol.
- 4) The UWB channel is approximately time invariant over the observational duration.

Based on the assumptions, the mean of  $\mathbf{y}_n$ , denoted as  $\bar{\mathbf{y}}$ , can be easily found from our definition of  $\mathbf{s}_{k,n,l}$ . Since noise has zero mean, we have [11], [13]

$$\bar{\mathbf{y}} = \frac{1}{M} \sum_{k,m,l} \mathbf{C}_{k,m,l} \mathbf{g}_k. \quad (6)$$

Then, the zero-mean data vector can be obtained by subtracting  $\bar{\mathbf{y}}$  from  $\mathbf{y}_n$

$$\mathbf{z}_n \triangleq \mathbf{y}_n - \bar{\mathbf{y}} = \sum_{k,l,m} \mathbf{C}_{k,m,l} \mathbf{g}_k \left( s_{k,m}(n+l) - \frac{1}{M} \right) + \mathbf{v}_n. \quad (7)$$

Let us define  $a_{k,m}(n+l) = s_{k,m}(n+l) - 1/M$ , and  $\mathbf{a}_{k,n,l} = [a_{k,0}(n+l), \dots, a_{k,M}(n+l)]$ . Then, we have  $\mathbf{a}_{k,n,l} = \mathbf{s}_{k,n,l} - (1/M)\mathbf{1}_M$ . Noticing that the vector  $\mathbf{s}_{k,n,l}$  is a unit vector with only one nonzero element occurring in one of its  $M$  positions with equal probability  $1/M$ , we can readily derive that  $E\{\mathbf{s}_{k,n,l}\} = (1/M)\mathbf{1}_M$  and  $E\{\mathbf{s}_{k,n,l}\mathbf{s}_{k,n,l}^H\} = (1/M)\mathbf{I}_M$ . Consequently,  $\mathbf{a}_{k,n,l}$  has zero mean and its covariance is given by [13]

$$\Phi \triangleq E\{\mathbf{a}_{k,n,l}\mathbf{a}_{k,n,l}^T\} = \frac{1}{M} \left( \mathbf{I}_M - \frac{1}{M}\mathbf{1}_M\mathbf{1}_M^H \right) \quad (8)$$

which is easily shown to have rank  $M-1$  since  $(1/\sqrt{M})\mathbf{1}_M$  is a unitary vector.

Rank deficiency of  $\Phi$  implies that elements in  $\mathbf{a}_{k,n,l}$  are correlated sources. We thus perform further transformation to obtain uncorrelated sources. Eigenvalue decomposition (EVD) on  $\Phi$  can be shown to take a form  $\Phi = \mathbf{B}_a \Lambda_a^2 \mathbf{B}_a^H$ , where  $\mathbf{B}_a$  is of  $M \times (M-1)$  and  $\Lambda_a$  is an  $(M-1) \times (M-1)$  diagonal matrix with all positive entries. Then, the correlated input vector can be decomposed as  $\mathbf{a}_{k,n,l} = \mathbf{B}_a \Lambda_a \tilde{\mathbf{a}}_{k,n,l}$ , with  $\tilde{\mathbf{a}}_{k,n,l}$  denoting a whitened input vector. Denote the  $(i, j)$ th element of  $\mathbf{B}_a$  as  $b_{i,j}$ , the  $j$ th diagonal element of  $\Lambda_a$  as  $\tilde{\lambda}_j$ , and the  $j$ th element of  $\tilde{\mathbf{a}}_{k,n,l}$  as  $\tilde{a}_{k,n,l}(j)$ , for  $i = 1, \dots, M$ ,  $j = 1, \dots, M-1$ . As a result, the zero-mean data vector in (7)

is rewritten with respect to the whitened inputs as the following

$$\mathbf{z}_n = \sum_{k,l,j} \mathbf{S}_{k,j,l} \mathbf{g}_k \tilde{a}_{k,n,l}(j) + \mathbf{v}_n \quad (9)$$

where we define a new code matrix for user  $k$ 's  $j$ th input  $\tilde{a}_{k,n,l}(j)$  during the  $(n+l)$ th symbol interval as

$$\mathbf{S}_{k,j,l} = \sum_{i=1}^M b_{i,j} \tilde{\lambda}_j \mathbf{C}_{k,i-1,l}, \quad \text{for } j = 1, \dots, M-1.$$

Equation (9) resembles a multirate CDMA system [7], where  $\mathbf{S}_{k,j,l}$  can be treated as a code matrix for the  $j$ th input in the whitened data vector  $\tilde{\mathbf{a}}_{k,n,l}$ . Let  $\mathbf{R} \triangleq E\{\mathbf{z}_n \mathbf{z}_n^H\}$  denote the covariance matrix of the zero-mean data vector. According to (9)

$$\mathbf{R} = \sum_{k,l,j} \mathbf{S}_{k,j,l} \mathbf{g}_k \mathbf{g}_k^H \mathbf{S}_{k,j,l}^H + \sigma_v^2 \mathbf{I}_\nu \quad (10)$$

where  $\sigma_v^2$  is the noise power. Express EVD of  $\mathbf{R}$  as

$$\mathbf{R} = [\mathbf{U}_s \quad \mathbf{U}_n] \begin{bmatrix} \Lambda_s + \sigma_v^2 \mathbf{I} & \mathbf{0} \\ \mathbf{0} & \sigma_v^2 \mathbf{I} \end{bmatrix} \begin{bmatrix} \mathbf{U}_s^H \\ \mathbf{U}_n^H \end{bmatrix}. \quad (11)$$

Suppose user 1 is the desired user. The subspace approach for estimating  $\mathbf{g}_1$  based on the orthogonal property between the desired signature and the noise subspace is proposed in [11] as follows

$$\hat{\mathbf{g}}_1 = \min_{\|\mathbf{g}\|=1} \sum_{j=1}^{M-1} \mathbf{g}^H \mathbf{S}_j^H \mathbf{U}_n \mathbf{U}_n^H \mathbf{S}_j \mathbf{g} \quad (12)$$

where  $\mathbf{S}_j \triangleq \mathbf{S}_{1,j,0}$  for a simple notation. Since the UWB system after transformation mimics a conventional CDMA system, a unique solution up to a multiplicative scalar is guaranteed under some identifiability conditions [7].

In practice,  $\mathbf{U}_n$  is not known *a priori*. It is usually obtained from the EVD of the sample covariance matrix  $\mathbf{R}$ . Due to effects of noise and finite samples, the dimension of the noise subspace has to be first determined by some detection techniques such as Akaike's information-theoretic criterion (AIC) [18], minimum description length (MDL) [19], or fixed-ratio detection [20]. Those techniques highly depend on the signal-to-noise ratio (SNR) and number of available samples [21]. If the dimension is correctly estimated, then the subspace method is one of the best second-order-based approaches. However, due to effects of noise and finite samples, the dimension of the noise subspace may be estimated incorrectly, resulting in degraded performance of the subspace method, as shown in [8]. By contrast, the POR technique [8] is able to asymptotically estimate the noise subspace without rank estimation, since  $\sigma_v^{2p} \mathbf{R}^{-p}$  can be decomposed for a positive integer  $p$  as

$$\sigma_v^{2p} \mathbf{R}^{-p} = \mathbf{U}_n \mathbf{U}_n^H + \mathbf{U}_s \text{diag} \left\{ \left( \frac{\sigma_v^2}{\lambda_i^2 + \sigma_v^2} \right)^p \right\} \mathbf{U}_s^H. \quad (13)$$

Clearly, each null basis has a unity weight, while the  $i$ th signal basis has a weight of  $(\sigma_v^2/\lambda_i^2 + \sigma_v^2)^p$ , which is less than 1, irrespective of the noise power. If we use  $\sigma_v^{2p} \mathbf{R}^{-p}$  with finite

$p$  to approximate the noise-subspace component  $\mathbf{U}_n \mathbf{U}_n^H$  in the subspace channel estimation (12), and noticing that scalar  $\sigma_v^{2p}$  will not affect the eigenvectors of a matrix, then the POR-based channel-estimation method is readily obtained as

$$\mathbf{g}_{\text{por}} = \arg \min_{\|\mathbf{g}\|=1} \sum_{j=1}^{M-1} \mathbf{g}^H \mathcal{S}_j^H \mathbf{R}^{-p} \mathcal{S}_j \mathbf{g}. \quad (14)$$

The solution to (14) is immediately obtained as the eigenvector of the summation matrix  $\sum_j \mathcal{S}_j^H \mathbf{R}^{-p} \mathcal{S}_j$  corresponding to its minimum eigenvalue  $\gamma_{\text{por}}$  (for convenience, we call it minimum eigenvector). Since  $(\sigma_v^2/\lambda_i^2 + \sigma_v^2)^p$  can converge to 0 for sufficiently large  $p$  and noticing (13), the proposed channel estimation in (14) converges to the subspace 1 as  $p \rightarrow \infty$ . Estimating the noise subspace from  $\mathbf{R}^{-p}$  has an obvious advantage. It eliminates a need to obtain the corresponding dimension and thus, mitigates the effects of noise and finite samples by a certain degree.

### B. Symbol Detection

Let us assume that the desired user's  $n$ th symbol is the desired symbol, i.e.,  $k = 1, l = 0$ . The Rake receiver can be readily constructed based on the estimated channel to detect the symbol that is reflected by the position of the only maximum value in  $\mathbf{a}_{1,n,0}$ . Therefore, we need to design  $M$  receivers  $\mathbf{f}_m (m = 1, \dots, M)$ , each detecting one element in  $\mathbf{a}_{1,n,0}$ . Then, outputs of the  $M$  receivers are compared and the index of the maximum element is determined. Considering that the information symbol takes values  $0, \dots, M-1$ , our detected symbol can be described as

$$\arg \max_{m \in \{1, \dots, M\}} \text{Re} \{ \mathbf{f}_m^H \mathbf{z}_n \} - 1.$$

According to (3), the  $m$ th rake receiver for the desired symbol can be found to be  $\mathbf{f}_m = \mathbf{C}_{1,m,0} \mathbf{g}_1$ . Invoking (5), the  $M$  Rake receivers can be shown to be

$$\mathbf{F}_{1,\text{Rake}} = [\mathbf{f}_1, \dots, \mathbf{f}_M] = \mathbf{H}_{1,0}. \quad (15)$$

## IV. PERFORMANCE ANALYSIS

We will derive the channel-estimation error and detection performance of the Rake receiver for our desired user in this section.

### A. Performance of the POR Channel Estimator

We start from an asymptotic performance of the proposed channel-estimation method, and then proceed to derive channel-estimation mean square error (mse) due to nontrivial noise and finite data samples.

1) *Asymptotic Performance:* Let the data covariance matrix be estimated as

$$\hat{\mathbf{R}} = \frac{1}{N} \sum_{n=1}^N \left( \mathbf{y}_n - \frac{1}{N} \sum \mathbf{y}_n \right) \left( \mathbf{y}_n - \frac{1}{N} \sum \mathbf{y}_n \right)^H. \quad (16)$$

Then, the asymptotic performance of the proposed approach can be obtained in the following.

*Proposition 1:* As  $\sigma_v^2 \rightarrow 0$  and  $N \rightarrow \infty$ ,  $\mathbf{g}_{\text{por}} \rightarrow \mathbf{g}_1$  holds for any fixed  $p$ . On the other hand, as  $p \rightarrow \infty$ , it also holds for any fixed  $\sigma_v^2$ .

*Proof:* As is known, the subspace channel estimation (12) will yield a true channel vector  $\mathbf{g}_1$  as  $N \rightarrow \infty$ . On the other hand, according to (13), two asymptotic equivalences can be obtained as  $\lim_{\sigma_v^2 \rightarrow 0} \sigma_v^2 \mathbf{R}^{-p} = \mathbf{U}_n \mathbf{U}_n^H$ , for a finite  $p$ , and  $\lim_{p \rightarrow \infty} \sigma_v^2 \mathbf{R}^{-p} = \mathbf{U}_n \mathbf{U}_n^H$  for a fixed  $\sigma_v^2$ . Using these results and noticing (14), the proposition immediately follows. ■

Although the POR method asymptotically yields the true channel-estimation vector, finite noise power, finite power  $p$ , and finite  $N$  all cause the channel estimate to deviate from its perfect value. Next, we will analyze the effects of noise and  $N$  for a finite  $p$ .

2) *Noise-Induced Channel-Estimation Error:* We first study the effect of noise by assuming that  $N \rightarrow \infty$ . Let

$$\begin{aligned} \mathbf{A} &= \sum_{j=1}^{M-1} \mathcal{S}_j^H \mathbf{R}^{-p} \mathcal{S}_j \\ \mathbf{A}_0 &= \sum_{j=1}^{M-1} \mathcal{S}_j^H \mathbf{U}_n \mathbf{U}_n^H \mathcal{S}_j \\ \mathbf{A}_p &= \sum_{j=1}^{M-1} \mathcal{S}_j^H \mathbf{U}_s \mathbf{\Lambda}_s^{-p} \mathbf{U}_s \mathcal{S}_j. \end{aligned} \quad (17)$$

Since by (14) the estimated channel vector is the minimum eigenvector, applying (13),  $\mathbf{A}$  can be decomposed as

$$\sigma_v^{2p} \mathbf{A} = \mathbf{A}_0 + \sum_{j=1}^{M-1} \mathcal{S}_j^H \mathbf{U}_s \text{diag} \left\{ \left( \frac{\sigma_v^2}{\lambda_i^2 + \sigma_v^2} \right)^p \right\} \mathbf{U}_s^H \mathcal{S}_j. \quad (18)$$

Note that the minimum eigenvector of  $\mathbf{A}_0$  is exactly the desired channel  $\mathbf{g}_1$ . The second term on the right-hand side of (18) can be viewed as a perturbation to  $\mathbf{A}_0$  due to noise and is denoted as  $\delta \mathbf{A}_0$ . According to [22], the first-order perturbation of the minimum eigenvector, induced by noise and denoted as  $\delta \mathbf{g}_{\text{noise}}$ , is given by

$$\delta \mathbf{g}_{\text{noise}} \approx -\mathbf{A}_0^\dagger \sum_{j=1}^{M-1} \mathcal{S}_j^H \mathbf{U}_s \text{diag} \left\{ \left( \frac{\sigma_v^2}{\lambda_i^2 + \sigma_v^2} \right)^p \right\} \mathbf{U}_s^H \mathcal{S}_j \mathbf{g}_1.$$

It is observed that channel-estimation error is related to the ratio  $(\sigma_v^2/\lambda_i^2 + \sigma_v^2)^p$ . At low SNR, a larger  $p$  is necessary to achieve a smaller channel-estimation error. Since the ratio is a fractional number, theoretically speaking, good channel-estimation performance can be achieved for sufficiently large  $p$ , irrespective of noise power. At high SNR, we can assume that  $\sigma_v^2 \ll \lambda_i$  for each  $i$ . Then, the fractional term  $(\sigma_v^2/\lambda_i^2 + \sigma_v^2)^p$  can be expanded into Taylor series, resulting in the following simplified channel-estimation error

$$\delta \mathbf{g}_{\text{noise}} \approx -\sigma_v^{2p} \mathbf{A}_0^\dagger \mathbf{A}_p \mathbf{g}_1 + \mathcal{O}(\sigma_v^{2p+2}). \quad (19)$$

This result implies that  $\delta \mathbf{g}_1$  is at the order of  $O(\sigma_v^{2p})$ , which is much smaller than that obtained in the minimum-variance method [13] for a large  $p$ .

3) *Perturbation Error From Finite Data Length*: Now, we turn to the effect of data length  $N$  on the channel mse. A perturbation  $\delta \mathbf{R} = \hat{\mathbf{R}} - \mathbf{R}$  occurs due to finite  $N$ , according to (16). It will cause  $\mathbf{A}$  and then our POR solution perturbed. Here, we are interested in the perturbation of the minimum eigenvector of  $\mathbf{A}$ , which is indeed the perturbation of the channel estimate. Let  $\mathbf{g}_{\text{por}}$  denote the ideal POR channel estimate in the case of  $N \rightarrow \infty$ . Under a small-perturbation assumption (large  $N$ ), using Taylor's expansion up to the first order and according to (17), we have

$$\delta \mathbf{A} = - \sum_{j=1}^{M-1} \mathcal{S}_j^H \sum_{k=1}^p \mathbf{R}^{-k} \delta \mathbf{R} \mathbf{R}^{-(p-k)} \mathbf{R}^{-1} \mathcal{S}_j.$$

Due to  $\delta \mathbf{A}$ ,  $\mathbf{g}_{\text{por}}$  is perturbed as  $\tilde{\mathbf{g}}_{\text{por}}$ . If we denote the channel perturbation error from finite  $N$  as  $\delta \mathbf{g}_N \triangleq \tilde{\mathbf{g}}_{\text{por}} - \mathbf{g}_{\text{por}}$ , according to [22], we have

$$\delta \mathbf{g}_N \approx -(\mathbf{A} - \gamma_{\text{por}} \mathbf{I})^\dagger \delta \mathbf{A} \mathbf{g}_{\text{por}} \approx \sum_{j=1}^{M-1} \sum_{k=1}^p \mathbf{T}_{j,k} \delta \mathbf{R} \mathbf{t}_{j,k} \quad (20)$$

where  $\mathbf{T}_{j,k}$  and  $\mathbf{t}_{j,k}$  are deterministic quantities given by

$$\mathbf{T}_{j,k} = (\mathbf{A} - \gamma_{\text{por}} \mathbf{I})^\dagger \mathcal{S}_j^H \mathbf{R}^{-k}, \quad \mathbf{t}_{j,k} = \mathbf{R}^{-(p-k)} \mathbf{R}^{-1} \mathcal{S}_j \mathbf{g}_{\text{por}}.$$

Therefore, the covariance of  $\delta \mathbf{g}_N$  becomes

$$\text{Cov}_{\mathbf{g}_N} \approx \sum_{j=1}^{M-1} \sum_{k_1, k_2=1}^p \mathbf{T}_{j,k_1} E \{ \delta \mathbf{R} \mathbf{t}_{j,k_1} \mathbf{t}_{j,k_2}^H \delta \mathbf{R} \} \mathbf{T}_{j,k_2}^H \quad (21)$$

and the mse is equal to the trace of  $\text{Cov}_{\mathbf{g}_N}$ . Both are dependent on the weighted covariance of  $\delta \mathbf{R}$ , which can be obtained following similar procedures as those in [7] and [22] but noticing our current colored inputs. The results for  $\Psi(\Theta) = E \{ \delta \mathbf{R} \Theta \delta \mathbf{R} \}$  to be frequently used in our later discussions have been derived in the following proposition.

*Proposition 2*: If  $\mathbf{H}$  in (4) is partitioned into  $L$  subblocks as  $\mathbf{H} = [\mathbf{H}_1, \dots, \mathbf{H}_L]$ , with each subblock corresponding to one symbol irrespective of user, and data covariance is estimated from  $N$  independent data vectors as (16), then, for a real system (all quantities are real)

$$\begin{aligned} \Psi(\Theta) &= \frac{(N-1)^2}{N^3} \sum_{l=1}^L \frac{1}{M} \sum_{j=1}^M (\tilde{\mathbf{h}}_{l,j}^T \Theta \tilde{\mathbf{h}}_{l,j}) \tilde{\mathbf{h}}_{l,j} \tilde{\mathbf{h}}_{l,j}^T \\ &\quad - \frac{(N-1)^2}{N^3} \sum_{l=1}^L \text{tr}(\mathbf{H}_l \Phi \mathbf{H}_l^T \Theta) \mathbf{H}_l \Phi \mathbf{H}_l^T \\ &\quad - \frac{(N-1)^2}{N^3} \sum_{l=1}^L \mathbf{H}_l \Phi \mathbf{H}_l^T (\Theta + \Theta^T) \mathbf{H}_l \Phi \mathbf{H}_l^T \\ &\quad + \frac{N-1}{N^2} [\text{tr}(\mathbf{R} \Theta) \mathbf{R} + \mathbf{R} \Theta^T \mathbf{R}] + \frac{1}{N^2} \mathbf{R} \Theta \mathbf{R} \end{aligned} \quad (22)$$

while for complex channel and noise

$$\begin{aligned} \Psi(\Theta) &= \frac{(N-1)^2}{N^3} \sum_{l=1}^L \frac{1}{M} \sum_{j=1}^M (\tilde{\mathbf{h}}_{l,j}^H \Theta \tilde{\mathbf{h}}_{l,j}) \tilde{\mathbf{h}}_{l,j} \tilde{\mathbf{h}}_{l,j}^H \\ &\quad - \frac{(N-1)^2}{N^3} \sum_{l=1}^L \text{tr}(\mathbf{H}_l \Phi \mathbf{H}_l^H \Theta) \mathbf{H}_l \Phi \mathbf{H}_l^H \\ &\quad - \frac{(N-1)^2}{N^3} \sum_{l=1}^L \mathbf{H}_l \Phi \left[ \mathbf{H}_l^H \Theta \mathbf{H}_l \right. \\ &\quad \quad \left. + (\mathbf{H}_l^H \Theta \mathbf{H}_l)^T \right] \Phi \mathbf{H}_l^H \\ &\quad + \frac{N-1}{N^2} [\text{tr}(\mathbf{R} \Theta) \mathbf{R} + \mathbf{H} \mathcal{A} (\mathbf{H}^H \Theta \mathbf{H})^T \mathcal{A} \mathbf{H}^H] \\ &\quad + \frac{1}{N^2} \mathbf{R} \Theta \mathbf{R} \end{aligned} \quad (23)$$

where we have defined

$$\tilde{\mathbf{h}}_{l,j} = \mathbf{H}_l \tilde{\mathbf{e}}_{M,j}, \quad \tilde{\mathbf{e}}_{M,j} = \mathbf{e}_{M,j} - \frac{1}{M} \mathbf{I}_M, \quad \mathcal{A} = \mathbf{I}_L \otimes \Phi$$

for shorter notations.

*Proof*: See the Appendix.  $\blacksquare$

The results in Proposition 2 are applicable for any modulation level  $M$ . However, in the special case of  $M = 2$ , they can be simplified. Considering a real system, according to definition of  $\tilde{\mathbf{h}}_{l,j}$ , we have  $\tilde{\mathbf{h}}_{l,1} = -\tilde{\mathbf{h}}_{l,2}$ , for  $M = 2$ . According to (8),  $\Phi$  can be rewritten as  $\Phi = (1/2) \sum_{j=1}^M \tilde{\mathbf{e}}_{M,j} \tilde{\mathbf{e}}_{M,j}^T$ . Then, it follows that  $\mathbf{H}_l \Phi \mathbf{H}_l^H = (1/M) \sum_{j=1}^M \tilde{\mathbf{h}}_{l,1} \tilde{\mathbf{h}}_{l,1}^T$ , and  $\text{tr}(\mathbf{H}_l \Phi \mathbf{H}_l^H \Theta) = \tilde{\mathbf{h}}_{l,1}^T \Theta \tilde{\mathbf{h}}_{l,1} = \tilde{\mathbf{h}}_{l,2}^T \Theta \tilde{\mathbf{h}}_{l,2}$ . Using the results, it is found that the first two terms for computing  $\Psi(\Theta)$  in a real system cancel each other. Similar results can be also derived for a complex system without repetition here. Therefore, for a real system

$$\begin{aligned} \Psi(\Theta) &= - \frac{(N-1)^2}{N^3} \sum_{l=1}^L \mathbf{H}_l \Phi \mathbf{H}_l^T (\Theta + \Theta^T) \mathbf{H}_l \Phi \mathbf{H}_l^T \\ &\quad + \frac{N-1}{N^2} [\text{tr}(\mathbf{R} \Theta) \mathbf{R} + \mathbf{R} \Theta^T \mathbf{R}] + \frac{1}{N^2} \mathbf{R} \Theta \mathbf{R} \end{aligned}$$

while for complex channel and noise

$$\begin{aligned} \Psi(\Theta) &= - \frac{(N-1)^2}{N^3} \\ &\quad \times \sum_{l=1}^L \mathbf{H}_l \Phi \left[ \mathbf{H}_l^H \Theta \mathbf{H}_l + (\mathbf{H}_l^H \Theta \mathbf{H}_l)^T \right] \Phi \mathbf{H}_l^H \\ &\quad + \frac{N-1}{N^2} [\text{tr}(\mathbf{R} \Theta) \mathbf{R} + \mathbf{H} \mathcal{A} (\mathbf{H}^H \Theta \mathbf{H})^T \mathcal{A} \mathbf{H}^H] \\ &\quad + \frac{1}{N^2} \mathbf{R} \Theta \mathbf{R}. \end{aligned}$$

4) *Channel-Estimation Error Due to Noise and Finite  $N$* : Based on the above analysis, total channel-estimation error due to combined effects of noise and finite  $N$  can be computed.

*Lemma:* For small  $\sigma_v^2$  and large  $N$ , the channel-estimation error is approximated by

$$E\{\|\tilde{\mathbf{g}} - \mathbf{g}_1\|^2\} \approx \|\mathbf{g}_{\text{por}} - \mathbf{g}_1\|^2 + E\{\|\tilde{\mathbf{g}} - \mathbf{g}_{\text{por}}\|^2\} \quad (24)$$

where the first term is obtained from (19) and the second term by the trace of (21).

*Proof:* Noticing that  $(\tilde{\mathbf{g}} - \mathbf{g}_1) = (\mathbf{g}_{\text{por}} - \mathbf{g}_1) + (\tilde{\mathbf{g}} - \mathbf{g}_{\text{por}})$ ,  $E\{\|\tilde{\mathbf{g}} - \mathbf{g}_1\|^2\}$  is expanded to three terms. The cross term can be neglected because  $E\{\delta\mathbf{R}\} = \mathbf{0}$  leads to  $E\{\tilde{\mathbf{g}} - \mathbf{g}_{\text{por}}\} \approx \mathbf{0}$  according to (20). Then, the lemma immediately follows. ■

## B. Detection Performance

We first study performance of the ideal Rake receiver when channel and data covariance are perfectly known. Then, we investigate its sensitivity to sample size. The desired user's information symbol is contained in the data vector  $\mathbf{a}_{1,n,0}$  whose channel matrix is given by (5) after setting  $k = 1$  and  $l = 0$ . That channel matrix is the first subblock in matrix  $\mathbf{H}$  and has been defined as  $\mathbf{H}_1$  in our Proposition 2. We only focus on a real system although we will still use  $^H$  instead of  $^T$  for consistency next.

Let us separate the desired signal from interference in  $\mathbf{z}_n$  as  $\mathbf{z}_n = \mathbf{H}_1\mathbf{a}_{1,n,0} + \mathbf{u}_n$ , where  $\mathbf{u}_n$  includes ISI and MA interference (MAI), and is approximated as a Gaussian process for convenience of analysis. Assume information symbol 0 is transmitted. Then,  $\mathbf{z}_n = \tilde{\mathbf{h}}_{1,1} + \mathbf{u}_n$ . Denote  $M$  Rake receivers simply by  $\mathbf{f}_j$ , for  $j = 1, \dots, M$ . Then, detection becomes  $\{\mathbf{f}_1^H \mathbf{z}_n > \mathbf{f}_j^H \mathbf{z}_n, j = 2, \dots, M\} = \{\Delta\mathbf{f}_j^H \mathbf{z}_n > 0\}$ , where  $\Delta\mathbf{f}_j = \mathbf{f}_1 - \mathbf{f}_j$ . Define an  $(M-1)$ -dimensional random vector  $\mathbf{x}_n = \Delta\mathbf{F}^H \mathbf{z}_n$ , where  $\Delta\mathbf{F}$  contains all  $\Delta\mathbf{f}_j$  as columns. Since  $\mathbf{z}_n$  is assumed Gaussian distributed,  $\mathbf{x}_n$  is also Gaussian with a probability density function given as follows:

$$f_{\mathbf{x}} = \frac{e^{-\frac{1}{2}(\mathbf{x}_n - \Delta\mathbf{F}^H \tilde{\mathbf{h}}_{1,1})^H (\text{Cov}(\mathbf{x}))^{-1} (\mathbf{x}_n - \Delta\mathbf{F}^H \tilde{\mathbf{h}}_{1,1})}}{\sqrt{(2\pi)^{M-1} \det(\text{Cov}(\mathbf{x}))}}$$

where  $\text{Cov}(\mathbf{x}) = \Delta\mathbf{F}^H \mathbf{R}_{\text{int}} \Delta\mathbf{F}$ ,  $\mathbf{R}_{\text{int}} = \mathbf{R} - \tilde{\mathbf{h}}_{1,1} \tilde{\mathbf{h}}_{1,1}^H$ . Probability of detection error becomes  $\text{BER}_0 = 1 - \text{Prob}\{\mathbf{x}_n > \mathbf{0}\} = 1 - \int \dots \int_0^\infty f_{\mathbf{x}} d\mathbf{x}$ . It can be numerically evaluated. Similarly, the bit error rate (BER) for information symbol 1,  $\dots$ , symbol  $M-1$ , denoted as  $\text{BER}_1, \dots, \text{BER}_{M-1}$ , can be derived as above. Then, the average probability of error becomes  $\text{BER} = (1/M) \sum_{m=0}^{M-1} \text{BER}_m$ .

In the special case of  $M = 2$ , the BER results become

$$\text{BER}_0 = 1 - Q\left(-\frac{\Delta\mathbf{f}_1^H \tilde{\mathbf{h}}_{1,1}}{\sigma_1}\right) = Q\left(\frac{\Delta\mathbf{f}_1^H \tilde{\mathbf{h}}_{1,1}}{\sigma_1}\right)$$

and

$$\text{BER}_1 = 1 - Q\left(-\frac{\Delta\mathbf{f}_2^H \tilde{\mathbf{h}}_{1,2}}{\sigma_2}\right) = Q\left(\frac{\Delta\mathbf{f}_2^H \tilde{\mathbf{h}}_{1,2}}{\sigma_2}\right)$$

where  $\Delta\mathbf{f}_2 = \mathbf{f}_2 - \mathbf{f}_1 = -\Delta\mathbf{f}_1$ ,  $\sigma_j^2 = \Delta\mathbf{f}_j^H (\mathbf{R} - \tilde{\mathbf{h}}_{1,j} \tilde{\mathbf{h}}_{1,j}^H) \Delta\mathbf{f}_j$ , for  $j = 1, 2$ . Since in this special case,  $\mathcal{S}_1 =$

$(1/2)(\mathbf{C}_{1,0,0} - \mathbf{C}_{1,0,1})$ ,  $\mathbf{H}_1 = [\mathbf{C}_{1,0,0}\mathbf{g}_1, \mathbf{C}_{1,0,1}\mathbf{g}_1]$ , and  $\tilde{\mathbf{h}}_{1,1} = \mathbf{H}_1 \tilde{\mathbf{e}}_{2,j}$ , it can be seen that  $\tilde{\mathbf{h}}_{1,1} = \mathcal{S}_1 \mathbf{g}_1$ ,  $\tilde{\mathbf{h}}_{1,2} = -\tilde{\mathbf{h}}_{1,1}$ , and  $\sigma_1^2 = \sigma_2^2$ . We can conclude that  $\text{BER} = \text{BER}_0 = \text{BER}_1$ . Moreover, according to (15), we have  $\Delta\mathbf{f}_1 = 2\tilde{\mathbf{h}}_{1,1}$ . After examining  $\text{BER}_0$ , it is found that BER depends on the SINR of the receiver  $\Delta\mathbf{f}_1$ . The output SINR can be obtained as

$$\text{SINR} = \frac{|\Delta\mathbf{f}_1^H \tilde{\mathbf{h}}_{1,1}|^2}{\sigma_1^2} = \frac{\Delta\mathbf{f}_1^H \tilde{\mathbf{h}}_{1,1} \tilde{\mathbf{h}}_{1,1}^H \Delta\mathbf{f}_1}{\Delta\mathbf{f}_1^H \mathbf{R}_{\text{int}} \Delta\mathbf{f}_1}. \quad (25)$$

In practice, channel-estimation error exists due to noise and finite  $N$ . Considering that the estimated channel vector can be expressed as

$$\tilde{\mathbf{g}} = \mathbf{g}_1 + \delta\mathbf{g}_{\text{noise}} + \delta\mathbf{g}_N = \mathbf{g}_{\text{por}} + \delta\mathbf{g}_N$$

the perturbed version of  $\Delta\mathbf{f}_1$ , rippled from channel estimation, becomes  $\tilde{\Delta\mathbf{f}}_1 = 2\mathcal{S}_1 \mathbf{g}_{\text{por}} + 2\mathcal{S}_1 \delta\mathbf{g}_N$ . Note that  $\mathbf{g}_{\text{por}}$  is a fixed quantity containing noise-induced error while  $\delta\mathbf{g}_N$  is a random quantity. If we denote  $2\mathcal{S}_1 \mathbf{g}_{\text{por}}$  as  $\mathbf{m}$  and  $2\mathcal{S}_1 \delta\mathbf{g}_N$  as  $\delta\mathbf{m}$  for simple notations, then the perturbed SINR can be evaluated as

$$\widehat{\text{SINR}} \approx \frac{\mathbf{m}^H \tilde{\mathbf{h}}_{1,1} \tilde{\mathbf{h}}_{1,1}^H \mathbf{m} + E\{\delta\mathbf{m}^H \tilde{\mathbf{h}}_{1,1} \tilde{\mathbf{h}}_{1,1}^H \delta\mathbf{m}\}}{\mathbf{m}^H \mathbf{R}_{\text{int}} \mathbf{m} + E\{\delta\mathbf{m}^H \mathbf{R}_{\text{int}} \delta\mathbf{m}\}}. \quad (26)$$

All unperturbed terms in (26) can be evaluated using the covariance matrix and the desired user's codes. Each expectation in (26) is then computed as  $E\{\delta\mathbf{m}^H \mathbf{X} \delta\mathbf{m}\} = 4\text{tr}\{\mathcal{S}_1^H \mathbf{X} \mathcal{S}_1 \text{Cov}_{\mathbf{g}_N}\}$ , where  $\mathbf{X}$  may be replaced by  $\tilde{\mathbf{h}}_{1,1} \tilde{\mathbf{h}}_{1,1}^H$  or  $\mathbf{R}_{\text{int}}$  correspondingly, and  $\text{Cov}_{\mathbf{g}_N}$  can be evaluated by (21).

## V. NUMERICAL EXAMPLES

In this section, we show the performance of the proposed channel estimator in terms of channel mse, and the performance of the Rake receiver constructed from the estimated channel in terms of output SINR and BER. We also verify our analytical results by simulations. Comparisons of the proposed approach with data-aided (DA) and non-data-aided (NDA) ML methods described in [5] and the subspace method in various channel situations are included.

### A. Performance of the Proposed Approach

We consider a UWB system with  $N_c = 8$ ,  $N_f = 4$ , and  $M = 2$ . If not stated otherwise, eight equal-powered users are assumed in the system. Each user's TH codes and 16-path Gaussian channel spread over one frame are randomly generated. The received signal is the second derivative of the Gaussian function with pulsewidth equal to 0.7 ns [3]. Simulation results are based on 100 independent realizations. User 1 is assumed to be the desired user, and the receiver is assumed to be synchronized to the desired user.

1) *Channel-Estimation Error:* We first illustrate effects of noise and  $p$  on channel mse in the case of  $N = \infty$  in Fig. 1.

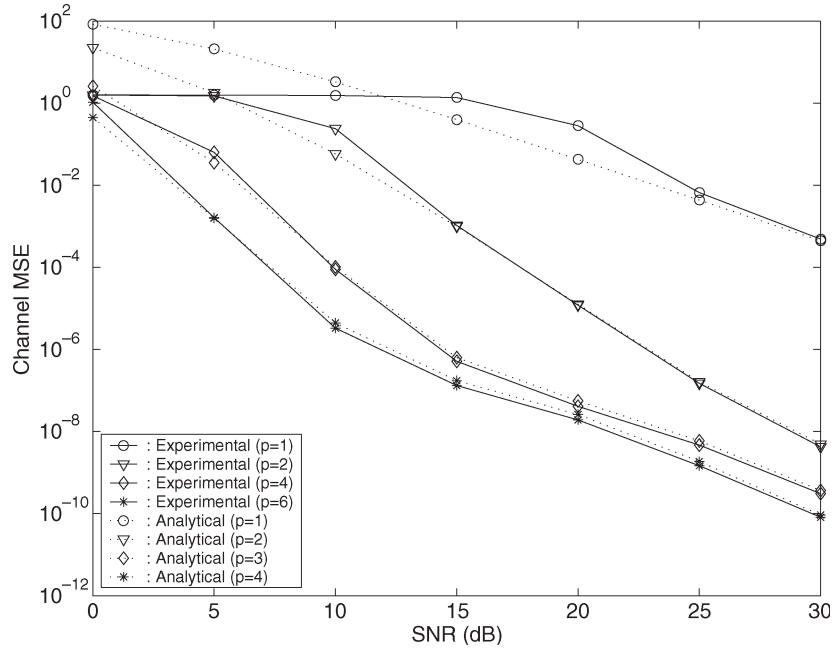


Fig. 1. Noise effect.

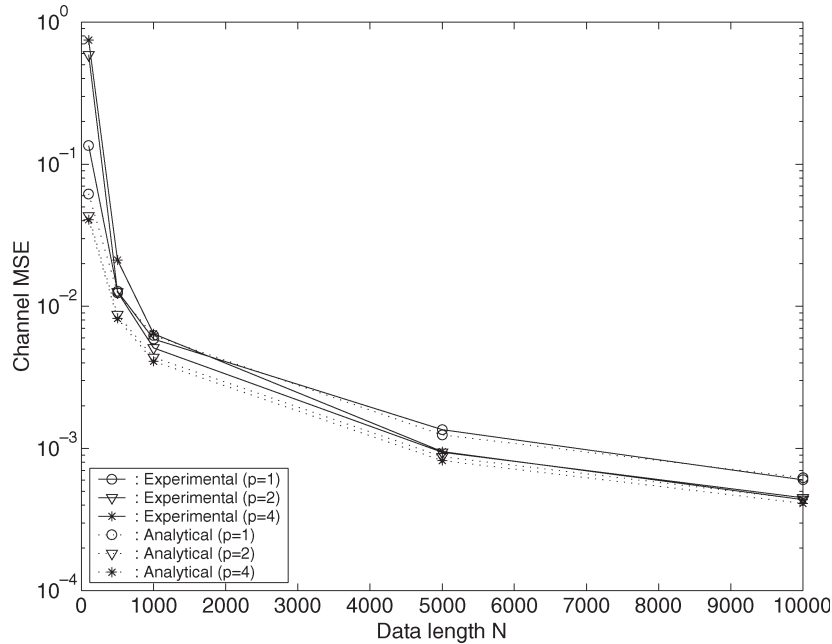


Fig. 2. Finite-data-sample-induced perturbation error.

Different  $p$ 's and various SNRs are considered. At very low SNR, a larger  $p$  is necessary to obtain good performance. By contrast, at high SNR, a smaller  $p$  is sufficient to yield a satisfactory performance with lower complexity. It can be seen that the proposed methods with  $p = 2$  and  $p = 4$  have most significant performance gains in environments with SNR of 10–25 dB. On the other hand, we also quantitatively examine the effect of noise on mse by plotting the analytical channel-estimation error in dotted lines for each  $p$ . We can observe that mses of the proposed method converge very well to their analytical values at high SNRs.

We then investigate the effect of data record length  $N$  on the channel perturbation error and compare results with corresponding analytical ones obtained from (21) in Fig. 2. The convergence of experimental perturbation errors to their analytical values is easily observed at large  $N$ . Moreover, either experimental or analytical perturbation errors are quite similar for all receivers with different  $p$  from  $N = 500$  and up, indicating that large  $p$  will not introduce substantial perturbation errors.

Finally, in Fig. 3, we illustrate the combined effect of SNR and  $N$  on the channel-estimation error, and compare it with the result in the lemma. We can see that the method with  $p = 1$

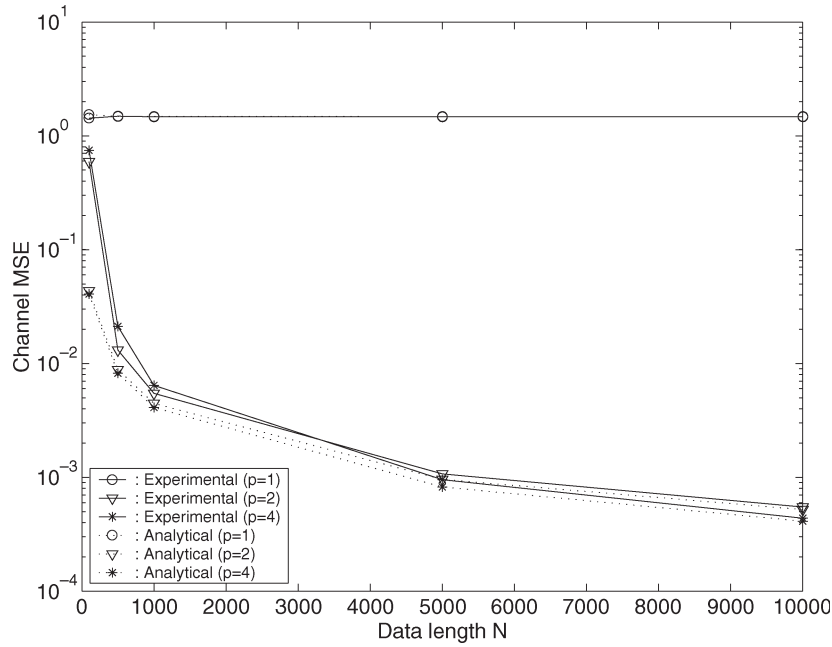


Fig. 3. Total channel-estimation error induced by both noise and finite  $N$ .

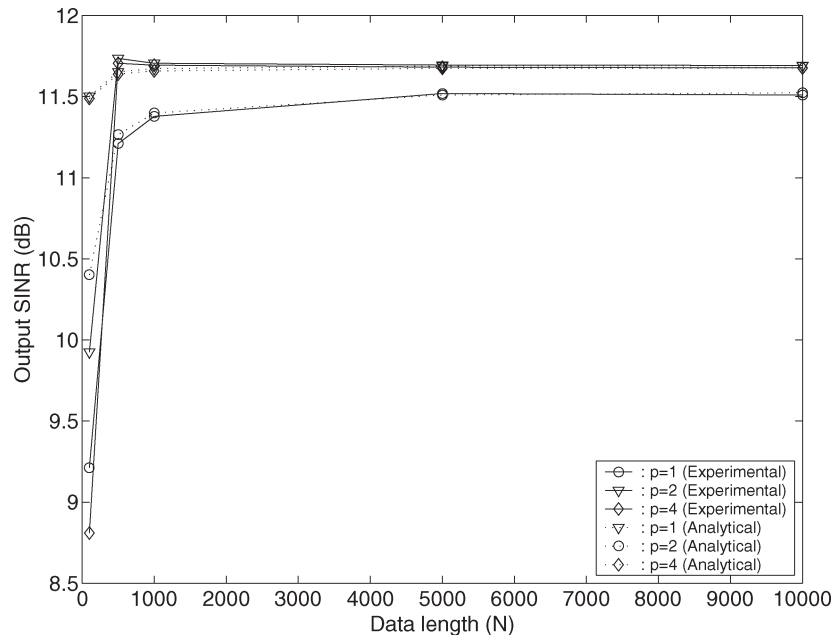


Fig. 4. Output SINR of the Rake receiver.

has the largest errors for all examined  $N$  due to large errors induced by noise. On the other hand, the perturbation error is the dominant error for the receivers with  $p = 2$ , and  $p = 4$  when  $N$  is not very large. As a result, the superiority of the proposed receivers with  $p = 4$  to that with  $p = 2$  is not observable even at very large  $N$  (e.g., 10 000). Based on this observation, we suggest to take  $p = 2$  in practice to achieve good performance and complexity tradeoff.

2) *Receiver's Performance:* We first show output SINR for each  $p$  in the presence of 15-dB noise in Fig. 4. Clearly, experimental SINR curves for all  $p$  converge to their corresponding analytical ones at large  $N$ . Moreover, the POR channel estimator with  $p = 2, 4$  shows similar performance and both are

superior to the POR channel estimator with  $p = 1$  due to better channel-estimation performance, as explained previously.

Fig. 5 then illustrates BER performance of the Rake receivers. Channel is first estimated based on 1000 data samples when a different  $p$  is applied. Then, Rake receivers are constructed from the estimated channels. We observe that Rake receivers with  $p = 2, 4$  have similar performance from 10 dB and up. Both are better than the receiver with  $p = 1$ . The analytical BER curve for the Rake receiver with  $p = 1$  is very consistent with its experimental counterpart. The discrepancy between the analytical and experimental BER curves for  $p = 2, 4$  at low SNR is caused by finite  $N$ , and may be caused by a violation of the Gaussian assumption on the MUI at high SNR.

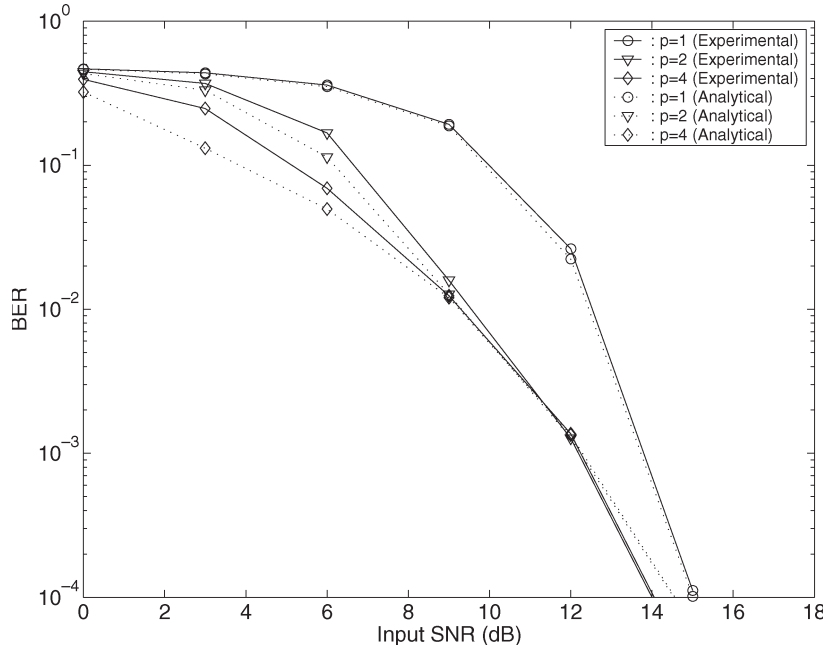


Fig. 5. BER performance of the Rake receiver.

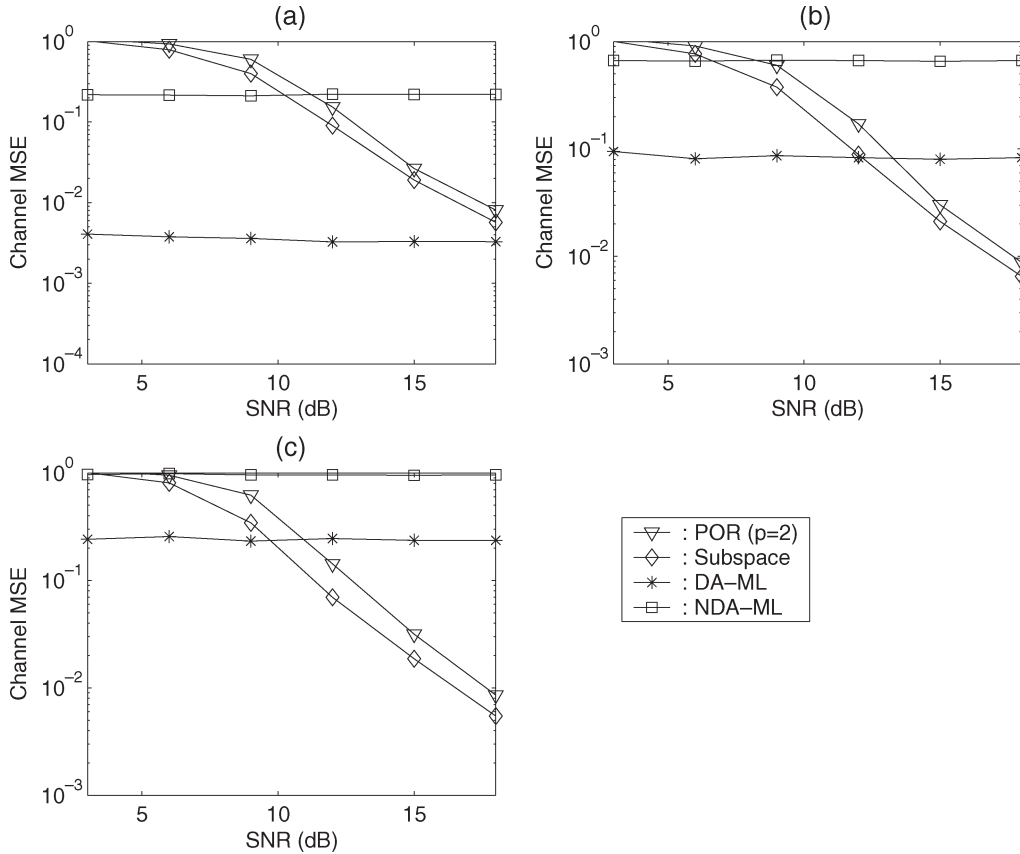


Fig. 6. Channel mse comparison for Gaussian channels: (a)  $K = 1$ ; (b)  $K = 5$ ; (c)  $K = 10$ .

**B. Comparison With Other Approaches**

Since [5] and [11] also consider channel estimation, a comparison with them is thus conducted and presented in this section. The POR method with  $p = 2$  is considered for comparison due to its best performance and complexity tradeoff

for moderate  $N$ , according to our simulation results in the previous section. The DA and NDA ML methods in [5] are termed as DA-ML and NDA-ML, respectively, and their Rake receivers with three fingers are used in the simulation. To implement the subspace method in [11], the dimension of the noise subspace is assumed perfectly known. Correspondingly,

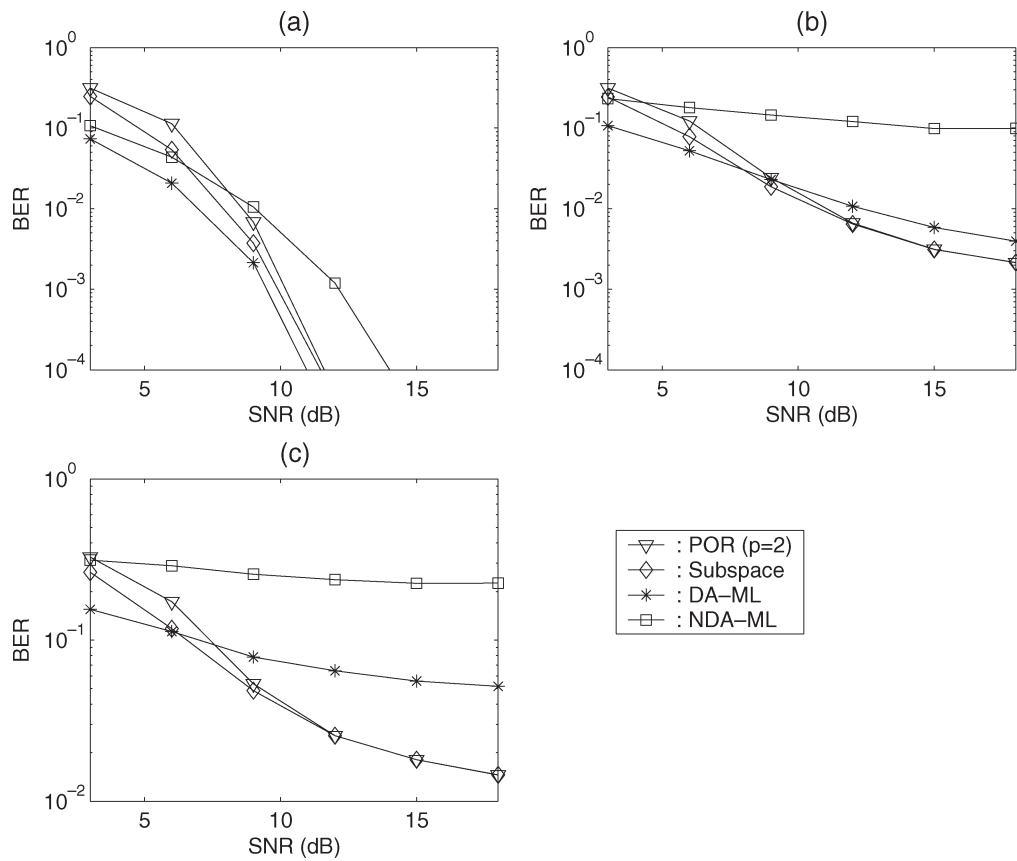


Fig. 7. BER comparison for Gaussian channels: (a)  $K = 1$ ; (b)  $K = 5$ ; (c)  $K = 10$ .

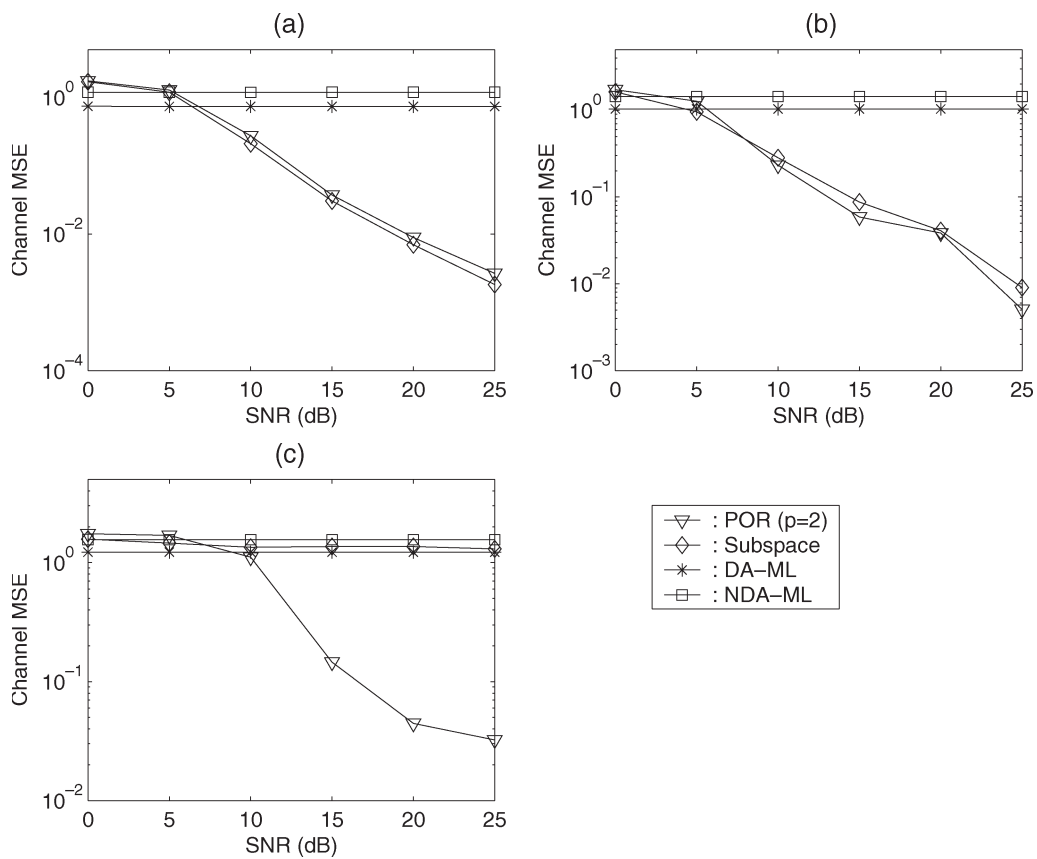


Fig. 8. Channel mse comparison based on channel model CM2: (a)  $K = 2$ ; (b)  $K = 5$ ; (c)  $K = 8$ .

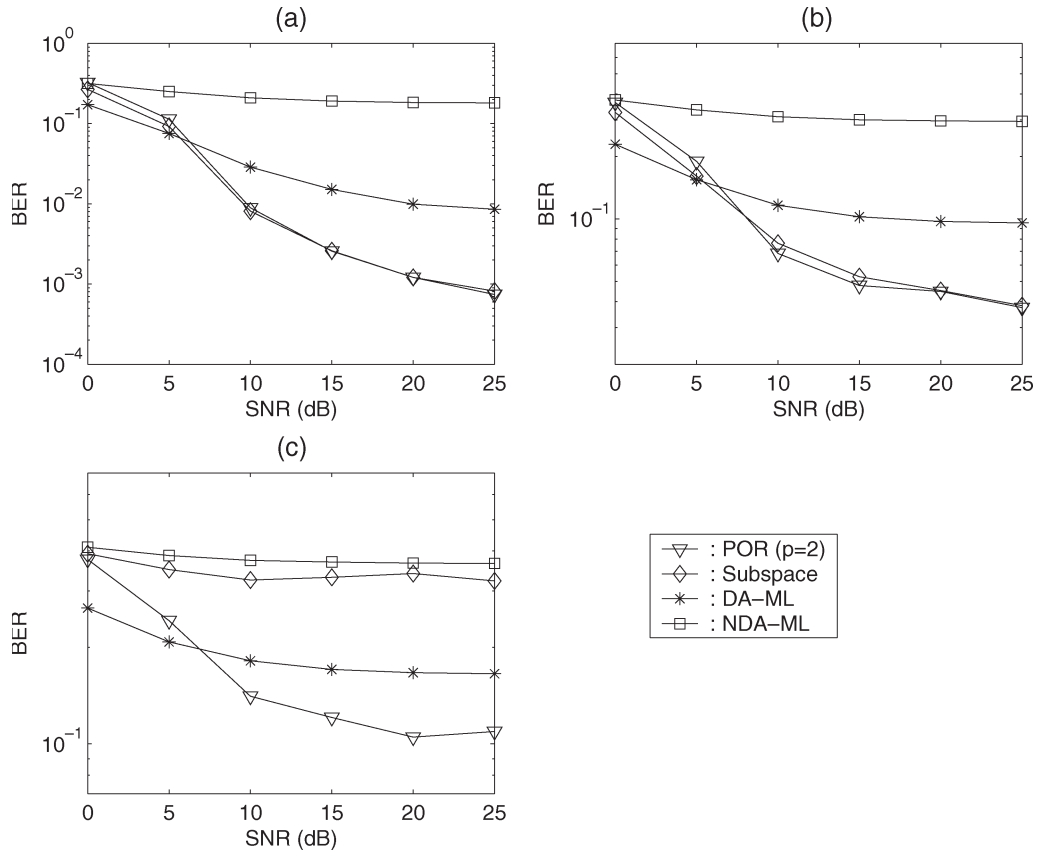


Fig. 9. BER comparison based on channel model CM2: (a)  $K = 2$ ; (b)  $K = 5$ ; (c)  $K = 8$ .

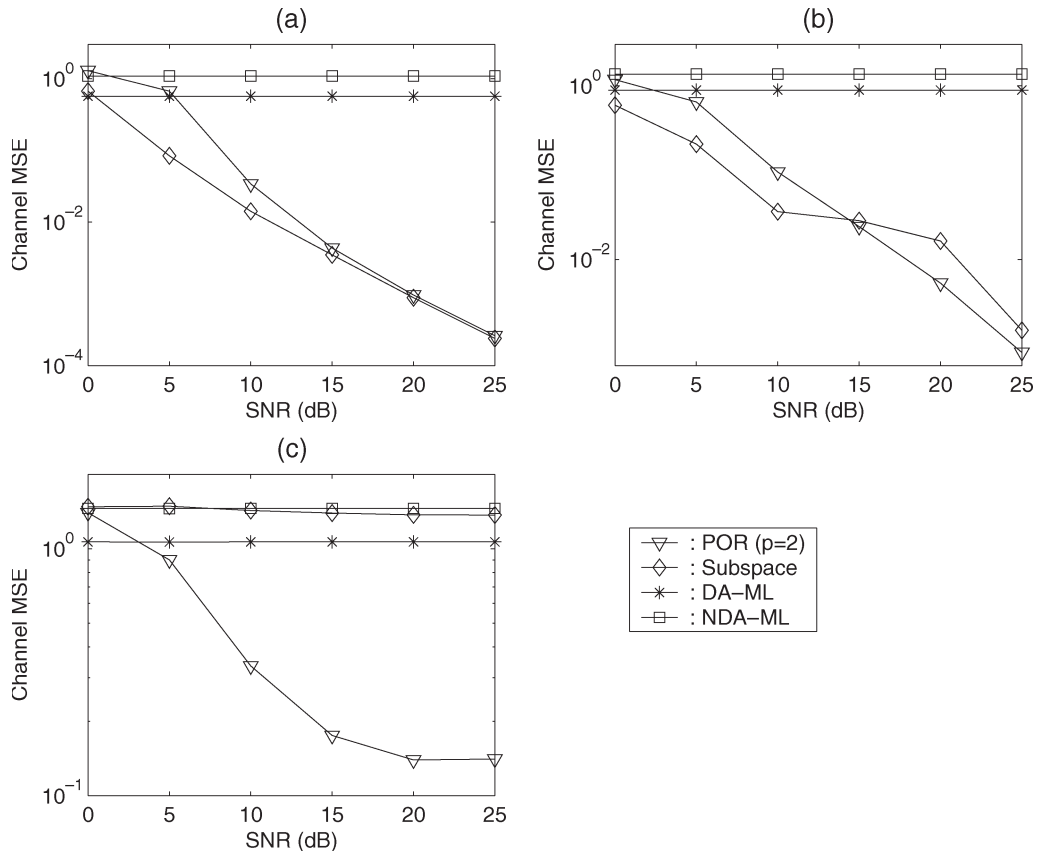


Fig. 10. Channel mse comparison based on channel model CM1: (a)  $K = 2$ ; (b)  $K = 5$ ; (c)  $K = 8$ .

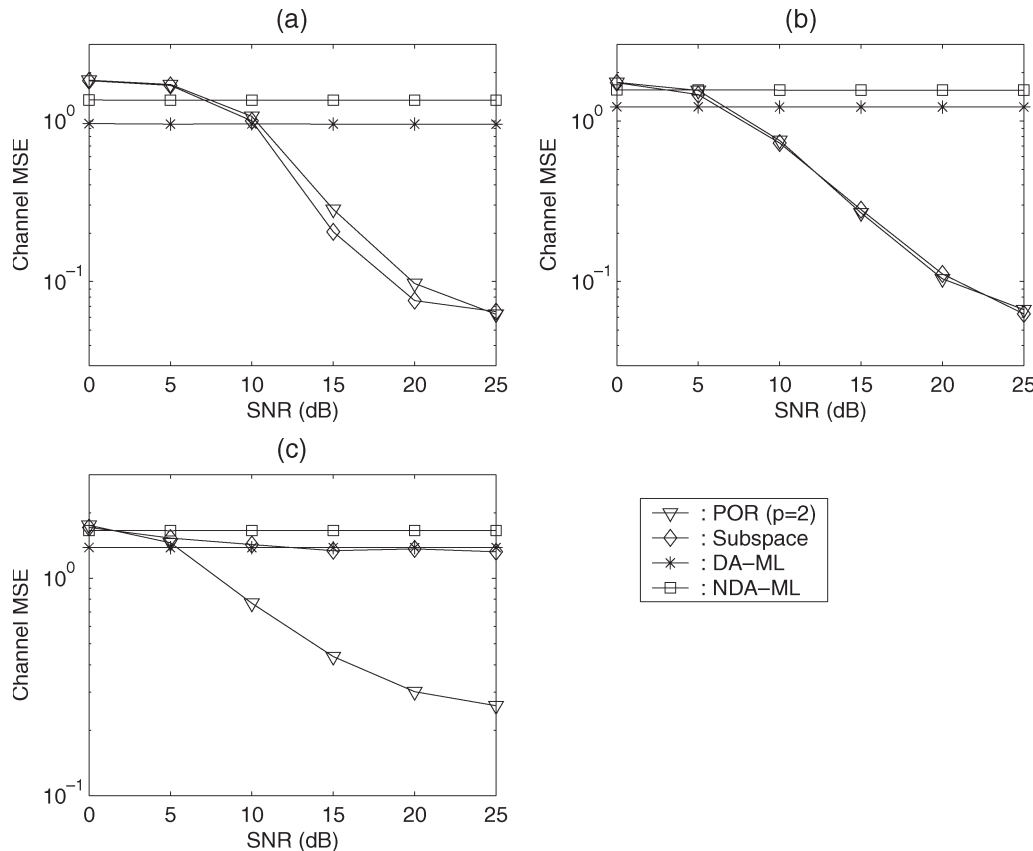


Fig. 11. Channel mse comparison based on channel model CM3: (a)  $K = 2$ ; (b)  $K = 5$ ; (c)  $K = 8$ .

the Rake receiver constructed from the subspace-based channel estimate is included for comparison.

The system parameters are taken as  $N_c = 10$  and  $N_f = 4$ . Each user experiences a different three-path channel, where the three paths are equally spaced at a five-chip interval. The desired user's three paths have gains 0.73, 0.67, and 0.35, as in [5]. The interfering users' path gains are randomly generated according to Rayleigh distribution and vary from run to run. Five hundred symbols are used for channel estimation. Instead of plotting delay and gain estimates separately, as in [5], we integrate them into a vector by associating each element of the vector with the gain of the channel at a particular pulse-level delay and filling 0's correspondingly if there is no path. The maximum delay of the desired user is assumed known to be a 15-pulse duration. The normalized mse for the integrated channel is then plotted in Fig. 6(a)–(c) for cases of  $K = 1$ ,  $K = 5$ , and  $K = 10$ , respectively. In the case of  $K = 1$ , DA-ML shows the best performance at low SNRs at the cost of using training data. In that case, DA-ML is close to the optimal receiver due to the absence of MUI and negligible ISI compared with noise power. However, at high SNR where ISI is dominant, the POR method with  $p = 2$ , though without the aid of training data, outperforms the training-based DA-ML and the blind NDA-ML greatly. For the case of  $K = 5$  or  $K = 10$ , due to significant MUI, the proposed method outperforms DA-ML significantly for most SNRs examined, and is clearly superior to NDA-ML for all SNRs examined. On the other hand, the POR method shows quite similar performance as the subspace method where noise-subspace dimension is assumed known.

The BER performance of different receivers is demonstrated in Fig. 7(a)–(c) for a different number of users, respectively. The POR method and the subspace method still have very similar performance. In the case of  $K = 1$ , the proposed Rake receiver shows very similar performance to the DA-ML Rake. In the case of  $K = 5$  and  $K = 10$ , the proposed Rake receiver shows better performance than either DA-ML or NDA-ML method due to better channel estimation for those cases. To summarize, the proposed method explicitly considers MAI in channel estimation, and thus achieves better performance than both DA-ML and NDA-ML approaches in [5]. The POR method can also achieve a similar performance as the subspace method, while without rank estimation of the noise subspace.

Next, we consider more realistic channels generated by three IEEE 802.15 channel models CM1, CM2, and CM3 [24]. CM1 is for line-of-sight (LOS) communication between 0 and 4 m, CM2 is for non-LOS (NLOS) between 0 and 4 m, and CM3 is for NLOS between 4 and 10 m. Those channel models modify the Saleh–Valenzuela model [25] to fit time-domain channel measurements. The delay spreads of CM1, CM2, and CM3 channels are truncated at 25, 40, and 80 ns for reduced complexity in channel estimation, yielding approximately 80% of the total energy on the average for each channel. After sampling every 1 ns, CM1, CM2, and CM3 channels then contain 25, 40, and 80 coefficients, respectively, which are much longer than those used before.

All simulation results in the following examples are based on 100 realizations. Different from previous examples, the multipath channels and TH codes are randomly generated for

each realization here. Considering the large delay spreads in CM1 to CM3 channels, we extend the received data vector  $\mathbf{y}_n$  to include more samples, i.e., from  $y(nP+1), \dots, y(nP+P+q)$ , instead of  $y(nP+1), \dots, y(nP+P)$ , as described in Section II. In all the following examples, 800 data symbols are used for channel estimation.

We first adopt CM2 for comparing both channel mean square error (mse) and receiver's BER among different approaches, since this model represents a very typical NLOS scenario. Fig. 8(a)–(c) plots channel mse versus input SNR for cases of two, five, and eight users, respectively. The system parameters are set as  $N_c = 5$  and  $N_f = 3$ . It is observed that the POR performs satisfactorily and outperforms the DA-ML and NDA-ML in all situations. Compared with the subspace method, POR shows similar performance in the two- and five-user situations, where the noise space contained in the data covariance matrix  $\mathbf{R}$  is still sufficiently large for estimating channel parameters. However, with eight users, there is no sufficient noise subspace in  $\mathbf{R}$ . Consequently, the subspace method degrades significantly. By comparison, the POR method still shows acceptable performance, which is much better than the subspace method. This implies that the POR method is more robust than the subspace method in the presence of a large number of interfering users. The BER performance of different receivers is demonstrated in Fig. 9(a)–(c), correspondingly. Similar conclusions can be drawn for the BER performance. Moreover, Figs. 8 and 9 suggest that BER results are quite consistent with the mse results, i.e., better channel-estimation performance will yield better detection performance. Based on this observation, we will present only channel-estimation results for channels generated by two other channel models CM1 and CM3 next, while omitting the BER performance for concise presentation.

Fig. 10(a)–(c) illustrates the channel mse for CM1. The system parameters are set to be  $N_c = 6$  and  $N_f = 2$ . Here, we adopt different  $N_c$  and  $N_f$  from the previous example, as we expect that the maximum number of users supported under identifiability conditions by the subspace method remains approximately the same as the previous example. We observe that the POR method performs equally as the subspace method in a lightly loaded system, while performs much better than others in an unfavorable situation with large number of interfering users. Fig. 11(a)–(c) illustrates the channel mse for CM3 in the presence of 2, 5, and 8 users, respectively. The system parameters are set to be  $N_c = 5$  and  $N_f = 4$  for the same reason mentioned above. A similar conclusion can be drawn even with long multipath channels.

To summarize, the proposed approach shows robust and acceptable performance in more realistic UWB channels. It is consistently better than both DA-ML and NDA-ML, and is superior to the subspace method in unfavorable situations with large number of interfering users.

## VI. CONCLUSION

In this paper, we have proposed a blind POR-based channel estimator for UWB communication systems employing PPM modulation. A Rake receiver is designed based on the estimated

channel for symbol detection. Asymptotic performance of both the channel estimator and receiver is derived based on perturbation theory. Extensive simulation results show satisfactory performance of the proposed scheme in various communication scenarios. The proposed approach shows consistent superiority over the ML method in most scenarios. It demonstrates similar performance as the subspace method in favorable communication environments with light loading, but significantly outperforms the subspace method in unfavorable situations with heavy loading.

## APPENDIX

### PROOF OF PROPOSITION 2

Since  $\Psi(\Theta) = E\{\delta\mathbf{R}\Theta\delta\mathbf{R}\}$  depends on  $\delta\mathbf{R} = \hat{\mathbf{R}} - \mathbf{R}$ , expanding the summation in (16), we obtain  $\hat{\mathbf{R}} = (1/N) \sum_n \mathbf{y}_n \mathbf{y}_n^H - (1/N^2) \sum_{n_1, n_2} \mathbf{y}_{n_1} \mathbf{y}_{n_2}^H$ . Substituting  $\mathbf{y}_n$  by  $\mathbf{z}_n + \bar{\mathbf{y}}$  according to (7), then, we have  $\hat{\mathbf{R}} = (1/N) \sum_n \mathbf{z}_n \mathbf{z}_n^H - (1/N^2) \sum_{n_1, n_2} \mathbf{z}_{n_1} \mathbf{z}_{n_2}^H$ , which is consistent with a typical covariance estimator. Due to zero mean and independence assumption on  $\mathbf{z}_n$ ,  $E\{\hat{\mathbf{R}}\} = (1 - 1/N)\mathbf{R}$ . Then,  $\Psi(\Theta)$  can be expanded into

$$\begin{aligned} \Psi(\Theta) &= E\left\{(\hat{\mathbf{R}} - \mathbf{R})\Theta(\hat{\mathbf{R}} - \mathbf{R})\right\} \\ &= E\{\hat{\mathbf{R}}\Theta\hat{\mathbf{R}}\} - \left(1 - \frac{2}{N}\right)\mathbf{R}\Theta\mathbf{R} \end{aligned} \quad (27)$$

where  $E\{\hat{\mathbf{R}}\Theta\hat{\mathbf{R}}\}$  is necessary for the evaluation of  $\Psi(\Theta)$ . For convenience, rewrite  $\hat{\mathbf{R}}$  as  $\hat{\mathbf{R}} = (N - 1/N^2) \sum_n \mathbf{z}_n \mathbf{z}_n^H - (1/N^2) \sum_{n_1 \neq n_2} \mathbf{z}_{n_1} \mathbf{z}_{n_2}^H$ . Noticing  $E\{\mathbf{z}_n\} = 0$ , we obtain

$$\begin{aligned} E\{\hat{\mathbf{R}}\Theta\hat{\mathbf{R}}\} &= \left(\frac{N-1}{N^2}\right)^2 \sum_{n_1, n_2} E\{\mathbf{z}_{n_1} \mathbf{z}_{n_1}^H \Theta \mathbf{z}_{n_2} \mathbf{z}_{n_2}^H\} \\ &\quad + \frac{1}{N^4} \sum_{n_1 \neq n_2} \sum_{n_3 \neq n_4} E\{\mathbf{z}_{n_1} \mathbf{z}_{n_2}^H \Theta \mathbf{z}_{n_3} \mathbf{z}_{n_4}^H\}. \end{aligned} \quad (28)$$

Invoking  $E\{\mathbf{z}_n\} = 0$  and independent assumption of  $\mathbf{z}_n$ , and noticing that only two cases:  $n_2 = n_3, n_1 = n_4$  but  $n_1 \neq n_2$ ;  $n_2 = n_4, n_1 = n_3$  but  $n_1 \neq n_2$ , will cause  $E\{\mathbf{z}_{n_1} \mathbf{z}_{n_2}^H \Theta \mathbf{z}_{n_3} \mathbf{z}_{n_4}^H\}$  to be nonzero, we can easily evaluate (28), resulting in (27) simplified as

$$\begin{aligned} \Psi(\Theta) &= \frac{(N-1)^2}{N^3} [E\{\mathbf{z}_n \mathbf{z}_n^H \Theta \mathbf{z}_n \mathbf{z}_n^H\} - \mathbf{R}\Theta\mathbf{R}] \\ &\quad + \frac{1}{N^2} \mathbf{R}\Theta\mathbf{R} + \frac{N-1}{N^3} \text{tr}(\mathbf{R}\Theta)\mathbf{R} \\ &\quad + \frac{N-1}{N^3} E\{\mathbf{z}_n \mathbf{z}_n^T\} \Theta^T (E\{\mathbf{z}_n \mathbf{z}_n^T\})^*. \end{aligned} \quad (29)$$

In order to complete the simplification of (29),  $E\{\mathbf{z}_n \mathbf{z}_n^H \Theta \mathbf{z}_n \mathbf{z}_n^H\} - \mathbf{R}\Theta\mathbf{R}$  and  $E\{\mathbf{z}_n \mathbf{z}_n^T\}$  are needed and will be derived next.

We first consider a real system. According to (7), we have

$$\mathbf{z}_n \mathbf{z}_n^T = \mathbf{H} \mathbf{a}_n \mathbf{a}_n^T \mathbf{H}^T + \mathbf{H} \mathbf{a}_n \mathbf{v}_n^T + \mathbf{v}_n \mathbf{a}_n^T \mathbf{H}^T + \mathbf{v}_n \mathbf{v}_n^T \quad (30)$$

$$\begin{aligned} \mathbf{z}_n^T \Theta \mathbf{z}_n &= \mathbf{a}_n^T \mathbf{H}^T \Theta \mathbf{H} \mathbf{a}_n + \mathbf{a}_n^T \mathbf{H}^T \Theta \mathbf{v}_n + \mathbf{v}_n^T \Theta \mathbf{H} \mathbf{a}_n \\ &\quad + \mathbf{v}_n^T \Theta \mathbf{v}_n. \end{aligned} \quad (31)$$

Considering zero mean of  $\mathbf{a}_n$  and  $\mathbf{v}_n$ , and  $\mathbf{R} = \mathbf{H} \mathbf{A} \mathbf{H}^T + \sigma_v^2 \mathbf{I}_\nu$  by (10), one can verify that

$$\begin{aligned} &E \{ \mathbf{z}_n \mathbf{z}_n^T \Theta \mathbf{z}_n \mathbf{z}_n^T \} - \mathbf{R} \Theta \mathbf{R} \\ &= E \{ \mathbf{H} \mathbf{a}_n \mathbf{a}_n^T \mathbf{H}^T \Theta \mathbf{H} \mathbf{a}_n \mathbf{a}_n^T \mathbf{H}^T \} + \sigma_v^2 \text{tr}(\Theta) \mathbf{H} \mathbf{A} \mathbf{H}^T \\ &\quad + \sigma_v^2 \mathbf{H} \mathbf{A} \mathbf{H}^T \Theta^T + \sigma_v^2 \Theta^T \mathbf{H} \mathbf{A} \mathbf{H}^T + \sigma_v^2 \text{tr}(\mathbf{A} \mathbf{H}^T \Theta \mathbf{H}) \mathbf{I}_\nu \\ &\quad + E \{ \mathbf{v}_n \mathbf{v}_n^T \Theta \mathbf{v}_n \mathbf{v}_n^T \} - \mathbf{H} \mathbf{A} \mathbf{H}^T \Theta \mathbf{H} \mathbf{A} \mathbf{H}^T - \sigma_v^4 \Theta. \end{aligned} \quad (32)$$

The first term can be further simplified as follows, after replacing  $\mathbf{H} \mathbf{a}_n$  by  $\sum_{l=1}^L \mathbf{H}_l \mathbf{a}_{n,l}$ , where  $E \{ \mathbf{a}_{n,l} \mathbf{a}_{n,l}^T \} = \Phi$ , and applying distribution of input

$$\begin{aligned} &E \{ \mathbf{H} \mathbf{a}_n \mathbf{a}_n^T \mathbf{H}^T \Theta \mathbf{H} \mathbf{a}_n \mathbf{a}_n^T \mathbf{H}^T \} \\ &= \sum_l E \{ \mathbf{H}_l \mathbf{a}_{n,l} \mathbf{a}_{n,l}^T \mathbf{H}_l^T (\mathbf{a}_{n,l}^T \mathbf{H}_l^T \Theta \mathbf{H}_l \mathbf{a}_{n,l}) \} \\ &\quad - \sum_l [\mathbf{H}_l \Phi \mathbf{H}_l^T \text{tr}(\Phi \mathbf{H}_l^T \Theta \mathbf{H}_l) \\ &\quad\quad + \mathbf{H}_l \Phi \mathbf{H}_l^T (\Theta + \Theta^T) \mathbf{H}_l \Phi \mathbf{H}_l^T] \\ &\quad + \mathbf{H} \mathbf{A} \mathbf{H}^T \text{tr}(\mathbf{H} \mathbf{A} \mathbf{H}^T \Theta) + \mathbf{H} \mathbf{A} \mathbf{H}^T (\Theta + \Theta^T) \mathbf{H} \mathbf{A} \mathbf{H}^T \end{aligned} \quad (33)$$

Also,  $E \{ \mathbf{v}_n \mathbf{v}_n^T \Theta \mathbf{v}_n \mathbf{v}_n^T \} = \sigma_v^4 \text{tr}(\Theta) \mathbf{I}_\nu + \sigma_v^4 (\Theta + \Theta^T)$  for a real AWGN as in [23, eq. (13)]. Applying these results into (32), replacing  $\mathbf{R}$  with  $\mathbf{H} \mathbf{A} \mathbf{H}^T + \sigma_v^2 \mathbf{I}_\nu$ , and considering  $\mathbf{a}_{n,l}$  takes  $M$  possible values with probability  $1/M$ , we obtain

$$\begin{aligned} &E \{ \mathbf{z}_n \mathbf{z}_n^T \Theta \mathbf{z}_n \mathbf{z}_n^T \} - \mathbf{R} \Theta \mathbf{R} \\ &= \sum_{l=1}^L \frac{1}{M} \sum_{j=1}^M (\tilde{\mathbf{h}}_{l,j}^H \Theta \tilde{\mathbf{h}}_{l,j}) \tilde{\mathbf{h}}_{l,j} \tilde{\mathbf{h}}_{l,j}^H \\ &\quad - \sum_l [\mathbf{H}_l \Phi \mathbf{H}_l^T \text{tr}(\Phi \mathbf{H}_l^T \Theta \mathbf{H}_l) \\ &\quad\quad + \mathbf{H}_l \Phi \mathbf{H}_l^T (\Theta + \Theta^T) \mathbf{H}_l \Phi \mathbf{H}_l^T] \\ &\quad + \text{tr}(\mathbf{R} \Theta) \mathbf{R} + \mathbf{R} \Theta^T \mathbf{R}. \end{aligned} \quad (34)$$

Considering  $\mathbf{R} = E \{ \mathbf{z}_n \mathbf{z}_n^T \}$  and substituting (34) into (29), we obtain (22).

For complex system, we can follow similar procedures as before. First, both  $\mathbf{z}_n \mathbf{z}_n^H$  and  $\mathbf{z}_n^H \Theta \mathbf{z}_n$  can be obtained as (30) and (31) with  $^T$  replaced by  $^H$ . Noticing that  $\mathbf{v}_n$  is zero-mean circularly symmetric Gaussian, we obtain

$$\begin{aligned} &E \{ \mathbf{z}_n \mathbf{z}_n^H \Theta \mathbf{z}_n \mathbf{z}_n^H \} - \mathbf{R} \Theta \mathbf{R} \\ &= E \{ \mathbf{H} \mathbf{a}_n \mathbf{a}_n^H \mathbf{H}^H \Theta \mathbf{H} \mathbf{a}_n \mathbf{a}_n^H \mathbf{H}^H \} + \sigma_v^2 \text{tr}(\Theta) \mathbf{H} \mathbf{A} \mathbf{H}^H \\ &\quad + \sigma_v^2 \text{tr}(\mathbf{A} \mathbf{H}^H \Theta \mathbf{H}) \mathbf{I}_\nu + E \{ \mathbf{v}_n \mathbf{v}_n^H \Theta \mathbf{v}_n \mathbf{v}_n^H \} \\ &\quad - \mathbf{H} \mathbf{A} \mathbf{H}^H \Theta \mathbf{H} \mathbf{A} \mathbf{H}^H - \sigma_v^4 \Theta \end{aligned} \quad (35)$$

where the first term can be similarly obtained as (33) but with different result after noticing that  $\mathbf{a}_{n,l}$  is a real vector, and  $E \{ \mathbf{v}_n \mathbf{v}_n^H \Theta \mathbf{v}_n \mathbf{v}_n^H \} = \sigma_v^4 \text{tr}(\Theta) \mathbf{I}_\nu + \sigma_v^4 \Theta$  for a complex

AWGN, as in [23, eq. (20)]. Therefore, one can verify that

$$\begin{aligned} &E \{ \mathbf{z}_n \mathbf{z}_n^H \Theta \mathbf{z}_n \mathbf{z}_n^H \} - \mathbf{R} \Theta \mathbf{R} \\ &= \sum_{l=1}^L \frac{1}{M} \sum_{j=1}^M (\tilde{\mathbf{h}}_{l,j}^H \Theta \tilde{\mathbf{h}}_{l,j}) \tilde{\mathbf{h}}_{l,j} \tilde{\mathbf{h}}_{l,j}^H \\ &\quad - \sum_l [\mathbf{H}_l \Phi \mathbf{H}_l^H \text{tr}(\Phi \mathbf{H}_l^H \Theta \mathbf{H}_l) \\ &\quad\quad + \mathbf{H}_l \Phi \mathbf{H}_l^H \Theta \mathbf{H}_l \Phi \mathbf{H}_l^H] \\ &\quad - \sum_l \mathbf{H}_l \Phi \mathbf{H}_l^T \Theta^T \mathbf{H}_l^* \Phi \mathbf{H}_l^H \\ &\quad + \text{tr}(\mathbf{R} \Theta) \mathbf{R} + \mathbf{H} \mathbf{A} \mathbf{H}^T \Theta^T \mathbf{H}^* \mathbf{A} \mathbf{H}^H. \end{aligned} \quad (36)$$

Since  $E \{ \mathbf{z}_n \mathbf{z}_n^T \} = \mathbf{H} \mathbf{A} \mathbf{H}^T$ ,  $(E \{ \mathbf{z}_n \mathbf{z}_n^T \})^* = \mathbf{H}^* \mathbf{A} \mathbf{H}^H$ , and substituting (36) into (29), (23) follows. ■

## REFERENCES

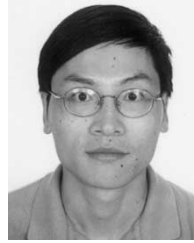
- [1] Federal Communications Commission News Release, *Revision of Part 15 of the Commission's Rules Regarding Ultra-Wideband Transmission Systems*, Feb. 14, 2002, Washington, DC. Available: ET Docket 98-153.
- [2] R. Fontana, A. Ameti, E. Richley, L. Beard, and D. Guy, "Recent advances in ultra wideband communications systems," in *Proc. Ultra Wideband Systems and Technologies (UWBST)*, Baltimore, MD, May 2002, pp. 129–133.
- [3] M. Z. Win and R. A. Scholtz, "Impulse radio: How it works," *IEEE Commun. Lett.*, vol. 2, no. 2, pp. 36–38, Feb. 1998.
- [4] —, "Characterization of ultra-wide bandwidth wireless indoor channels: A communication-theoretic view," *IEEE J. Sel. Areas Commun.*, vol. 20, no. 9, pp. 1613–1627, Dec. 2002.
- [5] V. Lottici, A. D'Andrea, and U. Mengali, "Channel estimation for ultra-wideband communications," *IEEE J. Sel. Areas Commun.*, vol. 20, no. 9, pp. 1638–1645, Dec. 2002.
- [6] C. J. Le Martret and G. B. Giannakis, "All-digital impulse radio with multiuser detection for wireless cellular systems," *IEEE Trans. Commun.*, vol. 50, no. 9, pp. 1440–1450, Sep. 2002.
- [7] Z. Xu, "Asymptotic performance of subspace methods for synchronous multirate CDMA systems," *IEEE Trans. Signal Process.*, vol. 50, no. 8, pp. 2015–2026, Aug. 2002.
- [8] Z. Xu, P. Liu, and X. Wang, "Towards closing the gap between MOE and subspace methods," in *Proc. Asilomar Conf. Signals, Systems, and Computers*, Pacific Grove, CA, Nov. 2002, pp. 689–693.
- [9] —, "Blind multiuser detection: From MOE to subspace methods," *IEEE Trans. Signal Process.*, vol. 52, no. 2, pp. 510–524, Feb. 2004.
- [10] X. Wang and H. V. Poor, "Blind equalization and multiuser detection in dispersive CDMA channels," *IEEE Trans. Commun.*, vol. 46, no. 1, pp. 91–103, Jan. 1998.
- [11] P. Liu, Z. Xu, and J. Tang, "Subspace multiuser receivers for UWB communication systems," in *Proc. IEEE Conf. Ultra Wideband Systems and Technologies*, Reston, VA, Nov. 16–19, 2003, pp. 116–120.
- [12] Z. Xu, P. Liu, and J. Tang, "A subspace approach to blind multiuser detection in ultra-wideband channels," *EURASIP J. Appl. Signal Process.: Special Issue on UWB—State of the Art*, vol. 2005, no. 3, pp. 413–425, Mar. 2005.
- [13] P. Liu, Z. Xu, and J. Tang, "Minimum variance multiuser detection for impulse radio UWB systems," in *Proc. IEEE Conf. Ultra Wideband Systems and Technologies*, Reston, VA, Nov. 16–19, 2003, pp. 111–115.
- [14] J. Tang, Z. Xu, and P. Liu, "Mean and covariance based estimation of multiple access UWB channels," in *Proc. IEEE Conf. Ultra Wideband Systems and Technologies*, Reston, VA, Nov. 16–19, 2003, pp. 458–462.
- [15] Z. Xu, J. Tang, and P. Liu, "Multiuser channel estimation for ultra-wideband systems using up to the second order statistics," *EURASIP J. Appl. Signal Process.: Special Issue on UWB—State of the Art*, vol. 2005, no. 3, pp. 273–286, Mar. 2005.
- [16] S. Verdú, *Multiuser Detection*. New York: Cambridge Univ. Press, 1998.
- [17] P. Lancaster and M. Tismenetsky, *The Theory of Matrices*, 2nd ed. San Diego, CA: Academic, 1985.
- [18] H. Akaike, "A new look at the statistical model identification," *IEEE Trans. Autom. Control*, vol. AC-19, no. 6, pp. 716–723, Dec. 1974.

- [19] J. Rissanen, "Modeling by shortest data description," *Automatica*, vol. 14, no. 5, pp. 465–471, 1978.
- [20] J. Tugnait and T. Li, "Blind asynchronous multiuser CDMA receivers for ISI channels using code-aided CMA," *IEEE J. Sel. Areas Commun.*, vol. 19, no. 8, pp. 1520–1530, Aug. 2001.
- [21] A. Liavas and P. Regalia, "On the behavior of information theoretic criteria for model order selection," *IEEE Trans. Signal Process.*, vol. 49, no. 8, pp. 1689–1695, Aug. 2001.
- [22] Z. Xu, "Perturbation analysis for subspace decomposition with applications in subspace-based algorithms," *IEEE Trans. Signal Process.*, vol. 50, no. 11, pp. 2820–2830, Nov. 2002.
- [23] —, "On the second-order statistics of the weighted sample covariance matrix," *IEEE Trans. Signal Process.*, vol. 51, no. 2, pp. 527–534, Feb. 2003.
- [24] *Channel Modeling Subcommittee Report Final*, Nov. 2002. IEEE P802.15-02/368r5-SG3a. [Online]. Available: <http://grouper.ieee.org/groups/802/15>
- [25] A. A. Saleh and R. A. Valenzuela, "A statistical model for indoor multipath propagation," *IEEE J. Sel. Areas Commun.*, vol. SAC-5, no. 2, pp. 128–137, Feb. 1987.



**Ping Liu** (S'00–M'03) received the B.S. and M.S. degrees in electronic engineering from Sichuan University, Chengdu, China, in 1990 and 1993, respectively, the M.Eng. degree in electrical and electronic engineering from Nanyang Technological University, Singapore, in 1999, and the Ph.D. degree in electrical engineering from University of California, Riverside, in 2004.

From 1993 to 1997, she worked as a Senior Software Engineer with International Software Development Company, Shenzhen, China. From April 1999 to August 1999, she worked as a Research Engineer with Kent Ridge Digital Labs, Singapore. Since August 2004, she has been an Assistant Professor with the Department of Electrical Engineering, Arkansas Tech University, Russellville. Her research interests are in the area of blind channel estimation and equalization, wireless multiuser communications, and digital signal processing.



**Zhengyuan Xu** (S'97–M'99–SM'02) received both the B.S. and M.S. degrees in electronic engineering from Tsinghua University, Beijing, China, in 1989 and 1991, respectively, and the Ph.D. degree in electrical engineering from Stevens Institute of Technology, Hoboken, NJ, in 1999.

From 1991 to 1996, he worked as an Engineer and Department Manager at the Tsinghua Unisplendour Group Corporation of Tsinghua University. Since 1999, he has been with the Department of Electrical Engineering, University of California, Riverside, as an Assistant Professor and then Associate Professor. His current research interests include detection and estimation theory, spread spectrum and ultra-wideband (UWB) wireless technology, multiuser communications, and ad hoc and wireless sensor networking.

Dr. Xu received the Outstanding Student Award and the Motorola Scholarship from Tsinghua University, and the Peskin Award from Stevens Institute of Technology. He also received the Academic Senate Research Award and the Regents' Faculty Award from University of California. He has served as a Session Chair, Technical Program Committee member and Publicity Chair for various international conferences. He is a member of the IEEE Technical Committee on Signal Processing for Communications, an Associate Editor for the IEEE TRANSACTIONS ON VEHICULAR TECHNOLOGY and the IEEE COMMUNICATIONS LETTERS.